EXPLORATION INTO THE SCOPE AND MECHANISM OF THE

PLATINUM-CATALYZED ACYLATION OF 2-(ARYLOXY)PYRIDINES

By

Jacob D. Guthrie

July 2019

Director of Thesis: Dr. Shouquan Huo

Major Department: Chemistry

Transition metal catalysts have played a key role in direct C-H bond functionalization. However, one main drawback of these reactions is that oxidants and additives are often required to regenerate the active catalyst, oxidize the substrates, or promote the reaction. These needed reagents can often add significant cost and safety concerns to the synthesis.

Recently the Huo group has discovered a unique platinum catalyzed acylation reaction to produce alpha-keto esters via C-H functionalization using ethyl chorooxoacetate, a cheap and readily accessible reagent. This reaction eliminated the need for any oxidants or additives and, more importantly, was free of any decarbonylation side reactions (see below). Further reaction optimization was performed to lower the catalyst loading. It was found that with the addition of potassium carbonate, strong acids that were produced during the C-H activation step (**B**) were neutralized thus allowing the catalyst to coordinate to the **1a** more readily. The range of the overall synthesis was explored using different acylating agents. Finally, Hammett analysis was used to study the substituent effects of this reaction. Experimental results will be reported, and the significance of these findings will be discussed.

EXPLORATION INTO THE SCOPE AND MECHANISM OF THE

PLATINUM-CATALYZED ACYLATION OF 2-(ARYLOXY)PYRIDINES

A Thesis

Presented to the Faculty of the Department of Chemistry

East Carolina University

In Partial Fulfillment of the Requirements for the Degree

Master of Science in Chemistry

by

Jacob D. Guthrie

July 2019

EXPLORATION INTO THE SCOPE AND MECHANISM OF THE

PLATINUM-CATALYZED ACYLATION OF 2-(ARYLOXY)PYRIDINES

By

Jacob D. Guthrie

APPROVED BY:

DIRECTOR OF

THESIS: _____

Shouquan Huo, PhD

COMMITTEE MEMBER: _____

Andrew Morehead, PhD

COMMITTEE MEMBER: _____

Brian Love, PhD

COMMITTEE MEMBER: _____

Baohong Zhang, PhD

CHAIR OF THE DEPARTMENT

OF CHEMISTRY: _____

Andrew Morehead, PhD

DEAN OF THE

GRADUATE SCHOOL: _____

Paul J. Gemperline, PhD

ACKNOWLEDGMENTS

TABLE OF CONTENTS

LIST OF TABLES

LIST OF FIGURES

LIST OF SCHEMES

LIST OF ABBREVIATIONS

C-H	Carbon-Hydrogen
C-C	Carbon-Carbon
C−Pt	Carbon-Platinum
Pt(II)	Platinum (II)
Pd(II)	Palladium (II)
Pt(IV)	Platinum (IV)
TBHP	tert-Butyl hydroperoxide
K_2CO_3	Potassium Carbonate
Na_2CO_3	Sodium Carbonate
Cs_2CO_3	Cesium Carbonate
CO_3	Carbonate
HCO_3	Bicarbonate
DIPEA	*N,N*-Diisopropylethylamine
Py	Pyridine
H_2O	Water
$CDCl_3$	Deuterated chloroform
CH_3	Methyl group

CF$_3$	Trifluoromethy group
OCH$_3$	Methoxy group
Et	Ethyl Group
o-	Ortho
m-	Meta
p-	Para
OH$^-$	Hydroxide ion
Cl$^-$	Chloride ion
KIE	Kinetic Isotope Effect
σ	Sigma
σ$_m$	Sigma meta
σ$_p$	Sigma para
σ$^+$	Sigma positive
σ$^-$	Sigma negative
ρ	Rho
HCl	Hydrochloric acid
^{0}C	Degrees centigrade
TLC	Thin Layer Chromatography

Cat. TON	Catalyst Turnover Number
GC	Gas Chromatography
PhCN	Benzonitrile
PhCl	Chlorobenzene
mmol	millimole
mL	milliliter
h	Hour
α	Alpha
β	Beta
γ	Gamma
δ	Chemical shift
NMR	nuclear magnetic resonance
MS	Mass spectrometry
Ppm	parts per million
Hz	hertz

CHAPTER 1: INTRODUCTION AND BACKGROUND

1.1 C-H activation and Pt

Transition metals have played a vital role in the evolution of C-H activation chemistry over the later part of the 20th century, and metals such as Pd(II) and Pt(II) have been especially influential[1,2]. Both transition metals have been key in the formation of several different types of organometallic complexes.[3-15] Many Pt-based catalytic systems have been studied for their ability to incorporate deuterium to hydrocarbons as the evidence of a catalytic C-H activation process.[9, 10, 15] However, it was the Shilov group in the late 1960's that maximized this finding[10]. The Shilov group reacted methane with water and convert the hydrocarbon to an alcohol[10] (**Scheme 1**).

Scheme 1. Proposed mechanism for Shilov Cycle
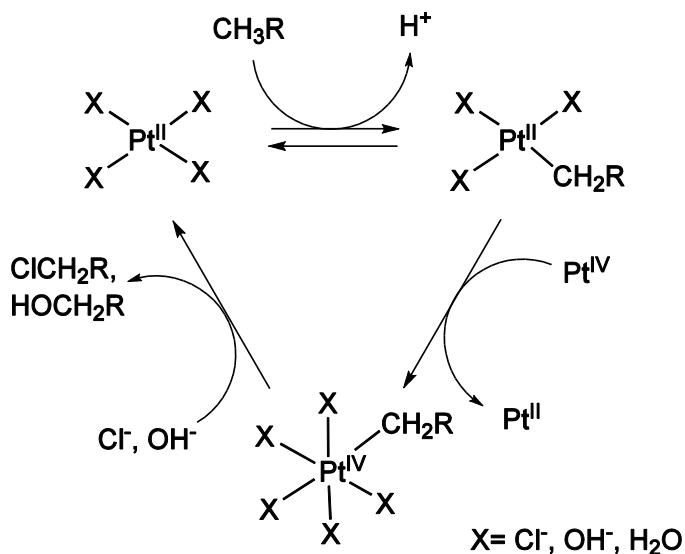
Primary steps of this reaction include: the electrophilic activation of the C-H bond, followed by oxidation of the Pt complex through nucleophilic oxidation of a hydrocarbon and, finishing with the nucleophilic attack performed by either an OH⁻ or Cl⁻ ligand to the Pt(IV) to regenerate the

Pt(II) catalyst. Inspired by the findings of the Shilov group Pd and Pt have been used as the catalyst to overcome complex organic synthesis problems[11-15]. However when looking at other transition metal catalysts the number of Pt based reactions is much smaller than Pd[16, 18], especially in regards to catalytic C-H activation and functionalization.[17] Current research in Pt(II) catalyst-based C-H functionalization has been looking at various issues challenging the scientific world. Some noteworthy findings include the ability to synthesize unique biological probes from complex substrates[19], functionalizing alkanes to various alcohols[14], and the oxy-functionalization of ethane[20]. These unique experiments highlight Pt(II)'s unique ability to overcome synthetic problems and demonstrate how insights can be gained into C-H activation mechanisms.

1.2 C-H activation and Mechanism Studies

When exploring C-H activation mechanisms there are a variety of quantitative techniques available. Often these techniques use reaction rates to help elucidate key mechanism information. Techniques such as Kinetic Isotope Effect (KIE) studies can often help elucidate the rate determining step of a reaction by labeling key hydrogens with their respective isotope in a compound and then examining how the bond cleavage or formation affects the overall reaction rate[21-23]. Another technique used is Hammett analysis. This technique observes how various electron donating/ electron withdrawing groups affect the overall rate of reaction compared to an unsubstituted substrate. Hammett analysis can help provide key mechanistic information by quantifying how various substituents can affect the build up of charge in a reaction mechanism[21-34].

Louis P. Hammett first proposed his findings in 1937 where he discussed how *meta* and *para* substituents of varying electronic nature would affect the ionization constant of benzoic

acid[26]. Hammett performed several experiments where he substituted benzoic acid with electron donating and electron withdrawing groups at the *meta* and *para* position and then compared the results to that of the unsubstituted group (**Scheme 2).** After setting arbitrary values to unsubstituted benzoic acid substituent constant ($\sigma = 0$) Hammett then compared the logarithm of the ionization constant of the substituted benzoic acid with the logarithm of the ionization constant of benzoic acid which then gave the value of the constant for that substituent (σ_m, σ_p).

Scheme 2 Ionization of benzoic acid in water

$R/R'=OH, NH_2, H$
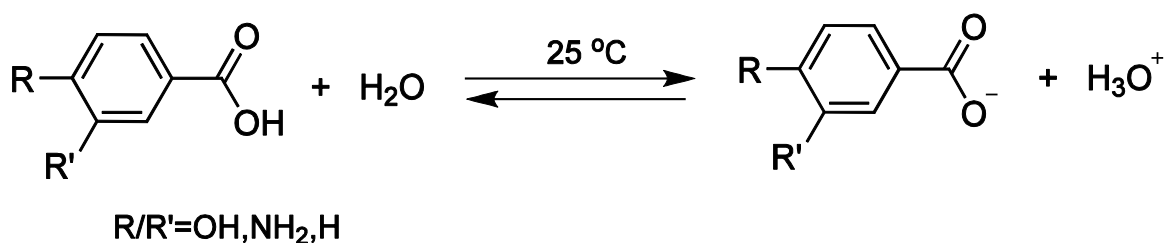
To account for error experienced in differing substrates (phenol, aniline, etc.) Hammett plotted the logarithm of the reaction rate for various substrates compared to the standard σ_m, σ_p derived from his previous experiment. He then went on to discuss how the change in free energy of activation of the varying substituents is proportional to the change in Gibbs free energy going against his previously reported notion of chemical kinetics[26]. From these experiments Hammett was able to create a liner free energy relationship relating reaction and equilibrium constants comparing the results to the ionization of benzoic acid to gauge sensitivity of substrate substitution (ρ).

The use of Hammett analysis for C-H activation mechanistic determination is quite common in current research[21-25, 27-29]. Some noteworthy findings include the use of Hammett analysis to help determine the charge build up seen in the rate determining step of direct Pd-

catalyzed arylation of five-membered heterocycles[25](**Scheme 3**). Hammett analysis was applied

through competition experiments of various substituted quinolines. Following the analysis, it was

found that a buildup of a positive charge occured during the key intermediate step. This then

helped the researchers determine their reaction followed an electrophilic metalation-

deprotonation.

Scheme 3 Competition reaction between quinoline derivatives and 8-(furan-2-yl)quinoline

R=NO$_2$, CF$_3$, OMe, NH$_2$
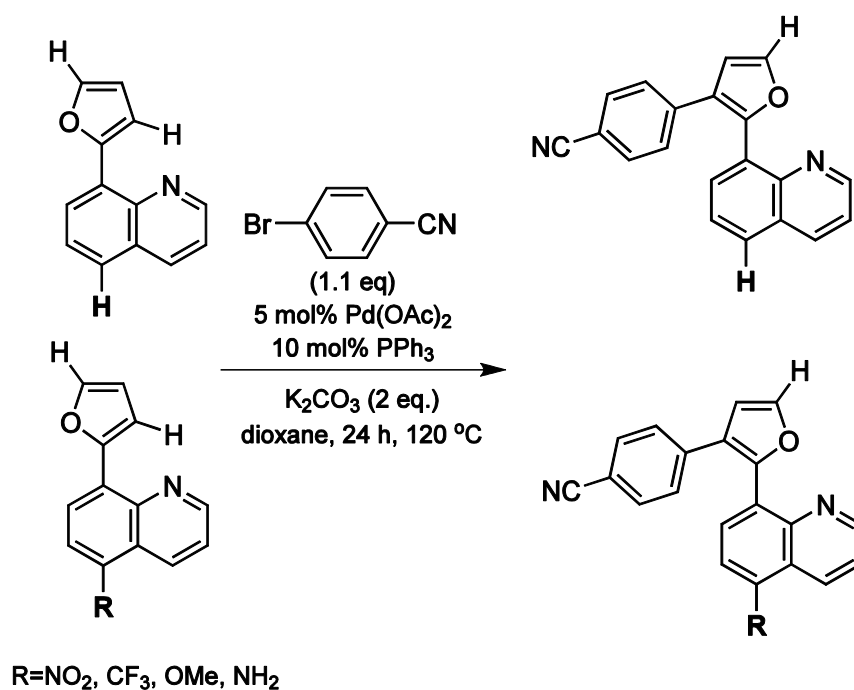
Other examples include the Re-catalyzed monoalkylation of phenols[22] where it was found that

the presence of electron withdrawing groups in the *meta* position related to the site of alkylation

sped up the rate of reaction which went against the hypothesized Friedel-crafts type mechanism

proposed (**Scheme 4**). Another study exploring Cobalt(III)-catalyzed hydroarylation of allenes

used Hammett analysis paired with computational experiments, KIE and kinetic order studies

helped propose a reversible catalytic cycle[31]. The Hammett analysis demonstrated an increase in

reaction rate when the arene is more electron deficient. This was indicated by the high

correlation (0.9185) and the ρ value plotted (+0.66) which demonstrated the build up of negative

charge in the reaction center that was then confirmed through the computational studies (**Scheme**

5). These experiments have been selected to highlight how Hammett analysis can further provide

information into reaction mechanism and demonstrate how insight can be gained into C-H

activation mechanism through the exploration of substituent effects.

Scheme 4 Re-Catalyzed Monoalkylation of substituted Phenols
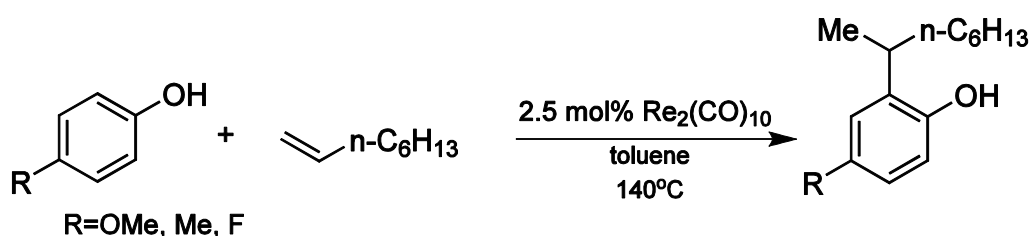
Scheme 5. Co(III)-Catalyzed Hydroarylation of Allenes
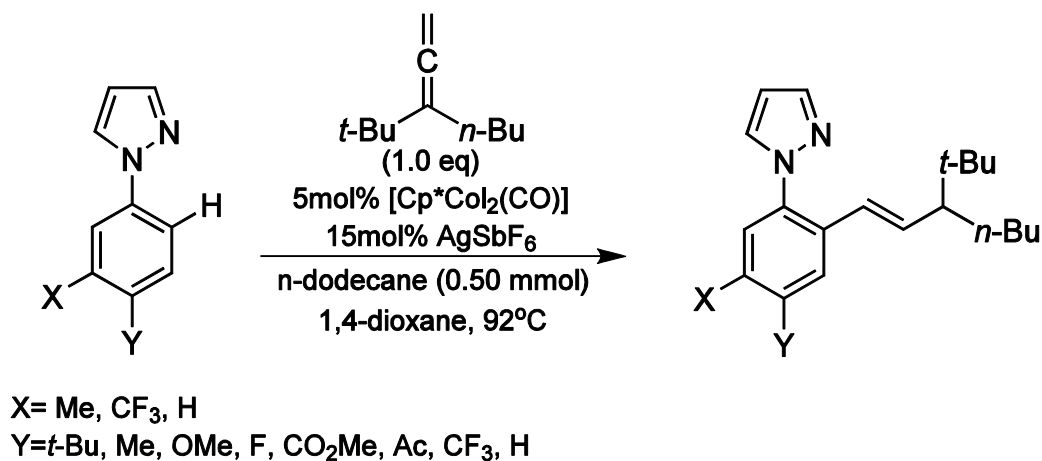
1.3 Research Relevance

The Huo group recently discovered a unique, platinum-catalyzed, direct C−H acylation

reaction (**Scheme 6**). This reaction does not make use of any oxidants like TBHP that is common

in similar transition metal catalyzed C-H functionalization reactions[4, 5]. By not having this

reagent in the reaction safety and fiscal concerns are lessened. Our group has continued to explore the scope of platinum catalyzed acylation reaction. With the use of ethyl chorooxoacetate an *ortho* acylated α-keto ester product has been produced (**Scheme 7**)[34]. This reaction is similar to the reaction previously performed with benzoyl chloride[4]. The primary difference is the presence of the second carbonyl group. Carbonyls are considered a vital part of many pharmaceutical products, and they can also be converted into different functional groups [4, 9]. It is also worth noting that this reaction avoids the decarbonylation side reaction that is often associated with the use of ethyl chlorooxoacetate. A previously reported reaction attempted to synthesize the α-keto ester using a Pd catalyst, ethyl glyoxylate as the acylating reagent and TBHP as the oxidant[35]. However, the reaction failed to obtain the α-keto ester but instead the decarbonylative products were formed.

Scheme 6. Published Pt catalyzed reaction of 2-phenoxypyridine with benzoyl chloride[4]
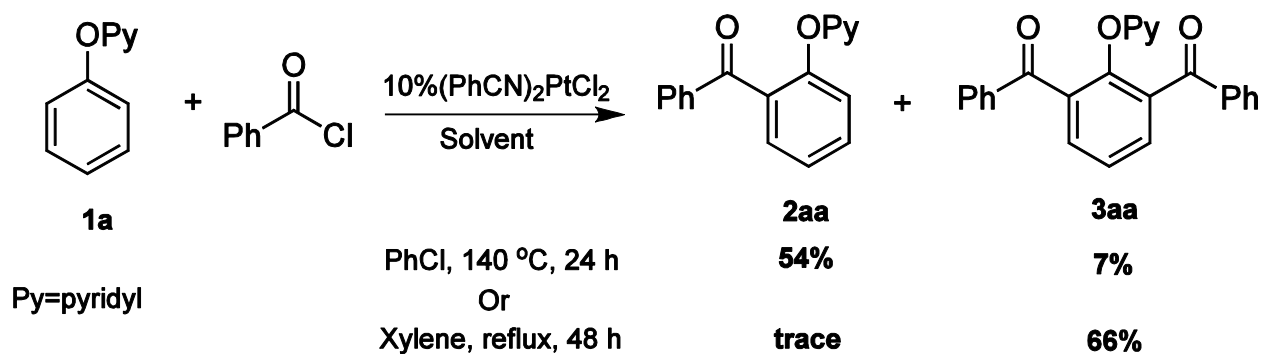
Scheme 7. Pt catalyzed direct ortho acylation reaction

1a-c

R=H,Cl,CH₃

2a-c
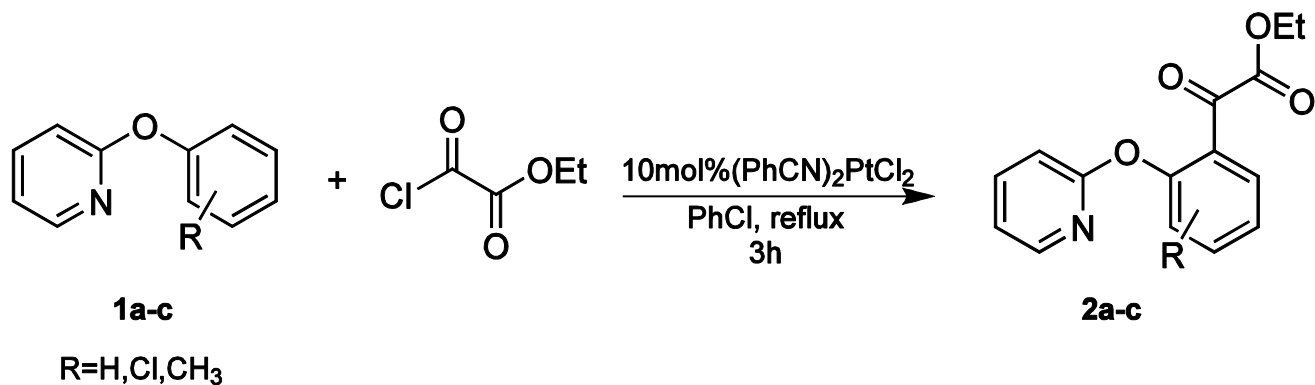
The proposed mechanism for the C−H acylation of a 2-(aryloxy)pyridine can be seen in **Scheme 8**. This mechanism proposes a coordination step between **1a** and the Pt(II) catalyst. The cyclometalation step then occurs and forms **B** which is then followed by the formal electrophilic addition of the acyl chloride (**2aa**). From there compound **C** is formed and the C-Pt bond is broken to form **D**. Then ligand exchange occurs and the catalyst either reenters the cycle or falls out of solution. This mechanism also includes the formation of a disubstituted product (**4aa**) Compound **C** may also rearrange to form **F** through intermediate **E**. Compound **F** then undergoes rearomatization through a deprotonation step. An acylated cycloplatinated compound **G** is then formed, which undergoes electrophilic addition of an acyl chloride. The C−Pt bond then dissociates and undergoes ligand exchange with **1a** to produce the diacylated product **4aa.** It is also possible that the monoacylated product **2aa** reenters the cycle to form the diacylated product.

It is assumed that the reaction mechanism for ethyl chorooxoacetate is the same as that for benzoyl chloride, this is due to similar results from both reagents and other similar acylation reactions. However it is the goal of this research to better understand the pathways of the Pt(II)-catalyzed C-H acylation reaction by expanding the reaction and mechanistic scope. by further establish the role that Pt plays in the acylation of 2-(aryloxy)pyridines.

Scheme 8. Published Mechanism for the Pt-Catalyzed Acylation Reaction
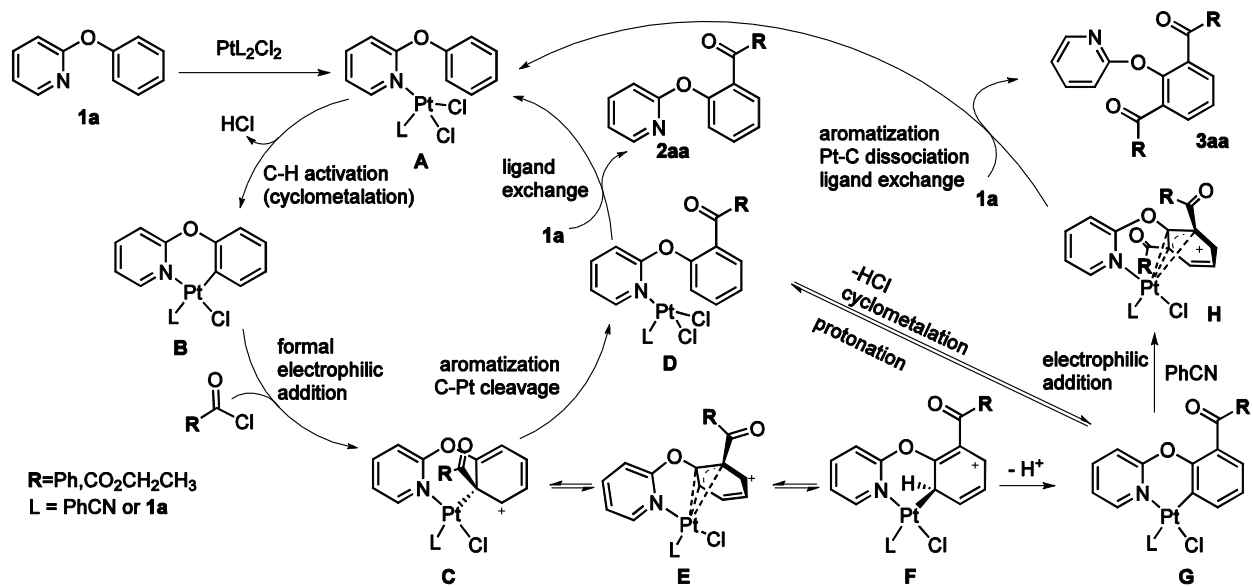
CHAPTER 2: RESEARCH OBJECTIVES

This research was carried out to accomplish three general goals regarding the platinum-catalyzed acylation of 2-(aryloxy)pyridines: reduction of catalytic loading, expansion of reaction scope via differing acylating groups, and mechanistic probing via Hammett analysis to gain insight into substitution effects. Using base, the catalytic cycle can become more efficient and alleviate the high costs associated with this acylation reaction. The use of different acyl chlorides further demonstrates the versatility of the acylation reaction.

An exploration was carried out to determine how varying substituents effected charge stability in the reaction and to gain further insight into the reaction mechanism. Using Hammett analysis, a linear free energy relationship was plotted to elucidate how differing substituents at the meta-, and para- position of the 2-(aryloxy)pyridine effect the acylation. The Hammett analysis was conducted via competing reactions where two substrates were combined into the same reaction vessel with minimal amounts of catalyst and acylating reagent. The difference in rate of conversion of various substituted 2-(aryloxy)pyridines was compared to that of a standard (**Scheme 9**). Further discussion of experimentation and findings are reported in Chapter 5.

Scheme 9 General Competing reaction for Hammett Analysis

R^1=H
R^2=EDG or EWG
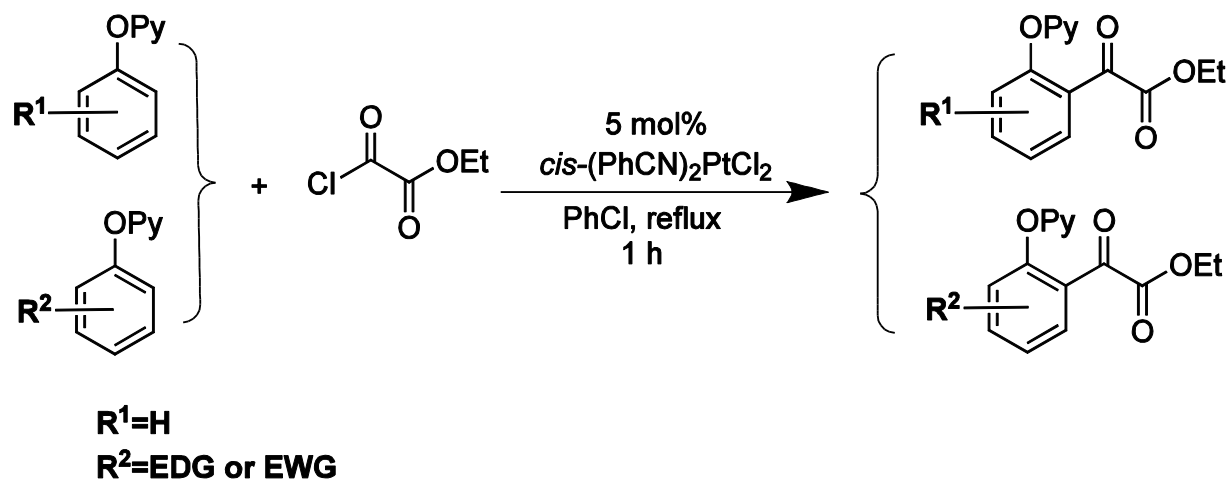
CHAPTER 3: REDUCTION OF CATALYTIC LOADING

3.1 Possible Role of Strong Acid in the Reaction

When considering the proposed mechanism shown in the previous chapter (**Scheme 8**) it
is important to note the formation of HCl during the C-H activation step. This acid is formed
from cyclometallation of 2-phenoxypyridine with cis-Pt(PhCN)$_2$Cl$_2$. The acid can bind to the
nitrogen of the 2-phenoxypyridine, which competes with the coordination of the ligand to the
catalyst. This obstacle could play a significant role in the previously reported need for 10%
catalyst loading. We hypothesized that if the HCl could be neutralized the overall catalytic
loading might be reduced to make the reaction not only more efficient but also more cost
effective.

3.2 Base Effect on the Reaction

To explore the potential reduction of catalytic loading through the neutralization of HCl
various bases were screened to determine their effectiveness. The initial reaction for the
screening used 2-naphthoxypyridine as the substrate, ethyl chlorooxoacetate as the acylating
reagent, and chlorobenzene as solvent. cis-(PhCN)$_2$PtCl$_2$ (5 mol%) was used as the catalyst and
the reaction was refluxed for 12 h (**Scheme10**). These conditions were chosen to mirror those
previously established for the acylation of aryloxy-pyridines to make alpha-keto esters[34] with
reaction times slightly modified to accommodate the lower catalytic load. Various bases were
selected to determine their overall effectiveness in neutralizing the acid while not hindering
overall reactivity. For this reason, bicarbonates where excluded due to the potential deactivation
of the acylating reagent. This reduction is a result of the H$_2$O that would form when neutralizing
the acid. The H$_2$O would convert the ethyl chloroOxoacetate to Oxalic acid monoethyl ester thus

preventing acylation. DIPEA was also used to examine if a bulky organic base could serve as an acid scavenger in the reaction. Due to its steric hindrance it appeared to be a reasonable choice to minimize the competing coordination to the platinum catalyst. Various equivalents of bases were examined, and reaction times were extended for reactions that produced less than 10% yield to ensure no further product formation. The results of this optimization can be found in **Table 1**

Scheme 10. General Base Optimization Reaction
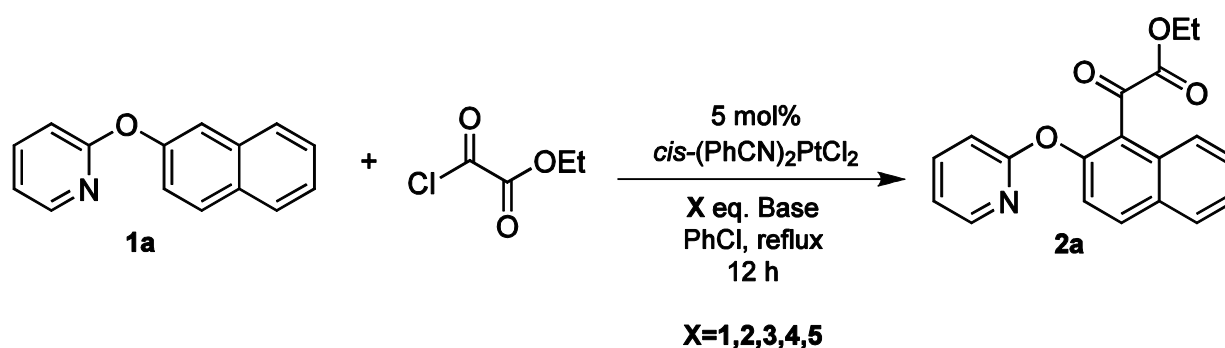
Table 1. Optimization of Base conditions for the Reaction of **1b.** using ethyl chloroxoacetate

Entry	Substrate	Base	Equiv.	Catalyst (%)	Reaction Time (h)	GC Yield (%)
1	1a	K_2CO_3	1	cis-Pt(PhCN)$_2$Cl$_2$ (5)	12	20
2	1a	K_2CO_3	2	cis-Pt(PhCN)$_2$Cl$_2$ (5)	12	25
3	1a	K_2CO_3	3	cis-Pt(PhCN)$_2$Cl$_2$ (5)	12	73
4	1a	K_2CO_3	3	cis-Pt(PhCN)$_2$Cl$_2$ (2.5)	24	<10
5	1a	K_2CO_3	4	cis-Pt(PhCN)$_2$Cl$_2$ (5)	12	28
6	1a	K_2CO_3	5	cis-Pt(PhCN)$_2$Cl$_2$ (5)	12	27
7	1a	Na_2CO_3	3	cis-Pt(PhCN)$_2$Cl$_2$ (5)	30	<10
8	1a	Cs_2CO_3	3	cis-Pt(PhCN)$_2$Cl$_2$ (5)	30	NR
9	1a	DIPEA	3	cis-Pt(PhCN)$_2$Cl$_2$ (5)	12	NR
10	1a	Pyridine	3	cis-Pt(PhCN)$_2$Cl$_2$ (5)	21	NR

[a] General conditions: Substrate (0.25 mmol), ethyl chlorooxoacetate (0.75 mmol), chlorobenzene (1.5 mL). K_2CO_3= potassium carbonate; Na_2CO_3 = sodium carbonate; Cs_2CO_3 = cesium carbonate; DIPEA = N,N-diisopropylethylamine. Yields found using Gas Chromatography using tetradecane (32.5 µL) as internal standard. All reactions were performed under argon

Following the optimization, it was found that 3 equivalents of K_2CO_3 was the optimal amount in lowing the overall catalytic loading. The 1 and 2 equivalents were not good because the amount of strong acid in the reaction vessel, which could also formed from hydrolysis of the acylating reagents through contacting with moisture, would form HCO_3^-. With acid still present in the reaction vessel the HCO_3^-. would then be react again forming CO_2 and H_2O thus hindering the reaction as previously mentioned. Because of the success with K_2CO_3, the same amount was also applied to the other bases that were tested. The Na_2CO_3 gave inferior results and Cs_2CO_3 inhibited the reaction. The use of pyridine also stopped the reaction, which can be explained by more favorable coordination of pyridine to the platinum catalyst than that of the substrate. Because of this more favorable coordination the Pt is more likely to undergo ligand exchange with the pyridine to form a stable pyridine complex and deactivate the platinum catalyst. This is further indicated by overall appearance of white-yellow precipitate forming immediately upon the addition of the base. The white solid was isolated and examined by ^{1}H NMR but full characterization was unsuccessful. DIPEA potentially acts as a reducing agent and follows a similar degradation pathway to that of pyridine. Though it is sterically hindered the potential is still there for coordination to the catalyst. The reaction mixture turned to a dark black color during this reaction and the starting material peak remained untouched throughout the entirety of the reaction. A large amount of black tar like substance remained at the bottom of the vessel indicating the Pt(II) catalyst had possibly been reduced to Pt(0), due to Pt coordinating to the base and deactivating.

It is worth noting that while performing the base optimization experiments no product degradation was observed on GC. This is significant since when performing the same acylation with the normal conditions (in the absence of a base) significant degradation of the product was

seen post 3 h of the reaction. This demonstrates that the presence of HCl could be a contributing factor in product degradation.

3.3 Application in Acylation Reactions

To fully gain insight into the scope of the reduced catalytic loading several substrates were further tested. The primary differences being the overall reaction time going from 3 h to12 h the addition of K_2CO_3 and the reduction of $(PhCN)_2PtCl_2$ loading from 10% to 5% versus the additive-free conditions (10% catalyst), (**Table 2**). The 5% $(PhCN)_2PtCl_2$ reaction was run for 12 h due to the optimized condition however, there is a possibility that each individual reaction may have completed long before this time. Each reaction was treated with pyridine for 1h following the reaction time to free the product from binding to the platinum to ensure the maximum recovery of the product. Products were also purified via column chromatography within 2 days of synthesis to avoid any possible degradation. Each product was examined using ^1H NMR and the resulting spectra were then compared to that of the previously reported results to ensure purity.

Table 2 shown below consists of the results. The resulting percent yields still favor the higher catalytic load in all cases with the exception of the 2-(naphthalen-2-yloxy)pyridine (**1a**). It is important to note a few things when comparing the two yields. It is also important to note that despite percent yield range difference (5%-15%) the overall loading is cut by 50% thus cutting the overall cost of this reaction by a significant amount.

Table 2 Comparison of Pt-catalyzed acylated products with 5% Pt(II) with K_2CO_3 against higher catalytic load and no base

^{a}5%= 12h, 79%
TON: 158
^{b}10%= 1h, 76%
TON: 76

^{a}5%= 12h, 73%
TON:146
^{b}10%= 1h, 84%
TON: 84

^{a}5%= 12h, 76%
TON:152
^{b}10%= 1h, 87%
TON: 87

^{a}5%= 12h, 70%
TON: 140
^{b}10%= 1h, 75%
TON: 75

^{a}5%= 12h, 69%
TON: 138
^{b}10%= 1h, 75%
TON: 75

^{a}5%= 12h, 70%
TON: 140
^{b}10%= 1h, 85%
TON: 85
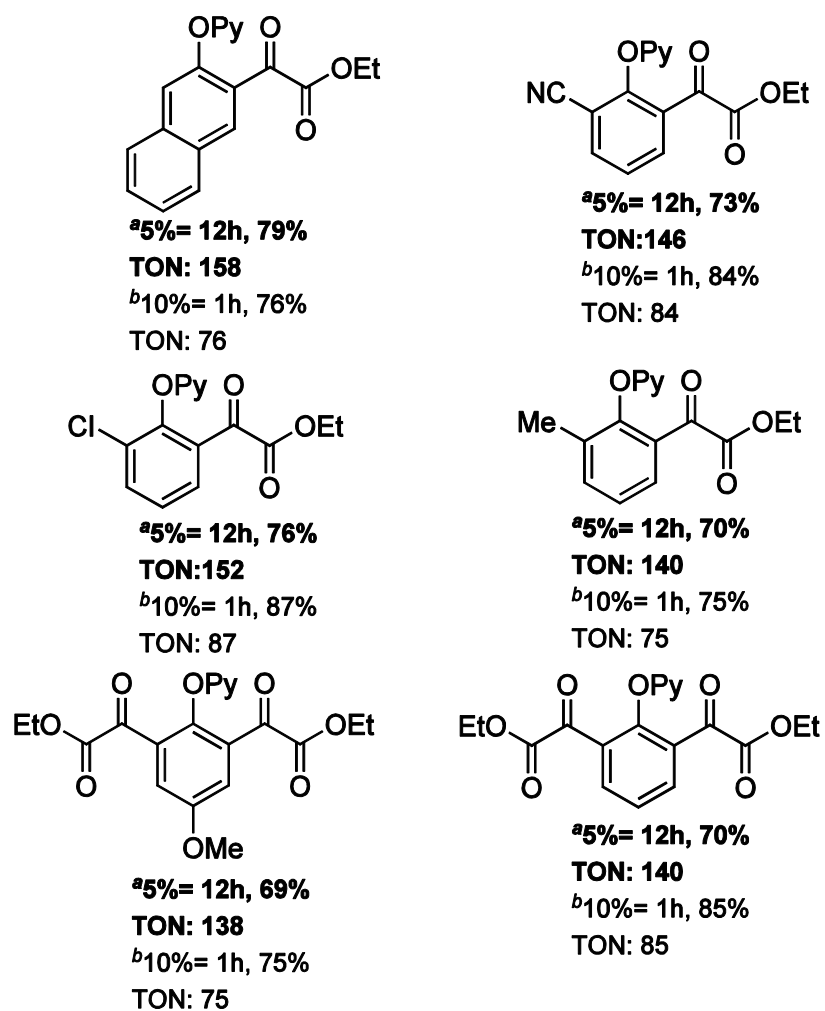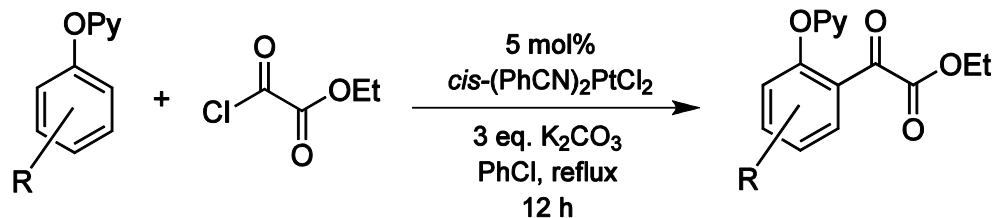
^{a} General conditions: 2-aryloxypyridine (0.5 mmol), ethyl chlorooxoacetate (1.5 mmol), *cis*-Pt(PhCN)$_2$Cl$_2$ (0.025 mmol),K$_2$CO$_3$ (1.5 mmol) chlorobenzene (3 mL), reflux. The reaction time was not optimized. Yields are isolated yields. ^{b}Previously reported reaction using *cis*-Pt(PhCN)$_2$Cl$_2$ (0.05 mmol)[34]

3.4 Acid-induced degradation of α -keto esters

To further explore the effect the K_2CO_3 had on the reaction, several control experiments (additive-free reaction) were performed. The first of these reactions aimed to test if the 5% $(PhCN)_2PtCl_2$ could cause the reaction to go to completion if given enough time. The 2-(naphthalen-2-yloxy)pyridine was used throughout the standardizing reactions due to its high yield during the base application as well as its use during the reaction optimization. (**Scheme 11**) After the 12 h of reaction it was noted that the reaction mixture was mostly black, indicating that the catalyst and product had most likely undergone degradation. Following workup, the overall reaction had a percent yield of 39%. This low overall percent yield compared to the base optimized reaction shows that the base is playing a significant role in the reaction and is necessary if the lower catalytic load is going to be used. However, this experiment alone does not demonstrate if degradation of product was the cause or the catalyst died before it could complete the reaction.

Scheme 11 Pt- catalyzed ortho acylation reaction using 5% catalytic load and no base
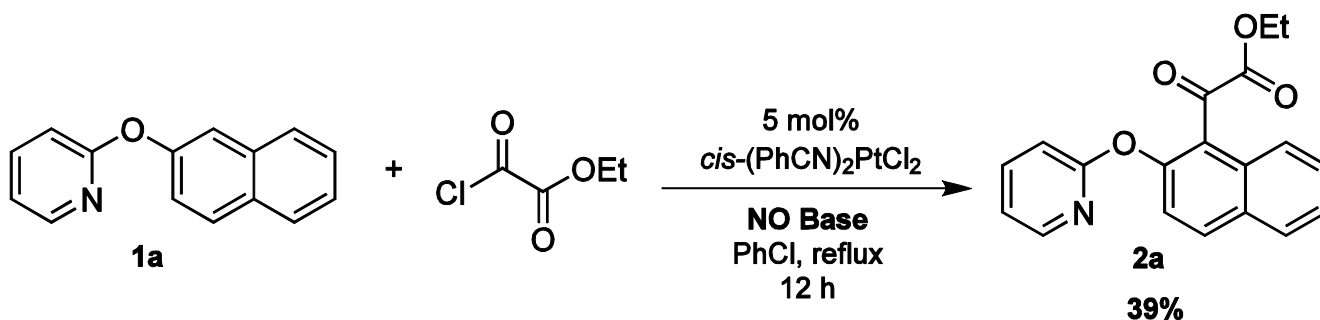
Following the findings from the lowered catalytic reaction, it was necessary to identify how the 10% $(PhCN)_2PtCl_2$ reaction would react when run for the 12h time frame (**Scheme 12**). It was noted at the end of the reaction that the reaction mixture was almost identical in appearance to that of that with lower catalyst loading. The TLC analysis of the reaction mixture showed trace amounts of starting material present and a significant spot that had stayed at the

bottom of the plate. Following workup, the overall reaction had a percent yield of 53%. Despite

this yield being higher than that with 5% (PhCN)$_2$PtCl$_2$, it still fell short of the previously

reported 76% when the reaction was run for only 1 h. It was then hypothesized that the 23%

difference is most likely attributed to product degradation by the strong acid produced in the

reaction.

Scheme 12 Pt- catalyzed *ortho* acylation reaction using 10% catalytic load and no base
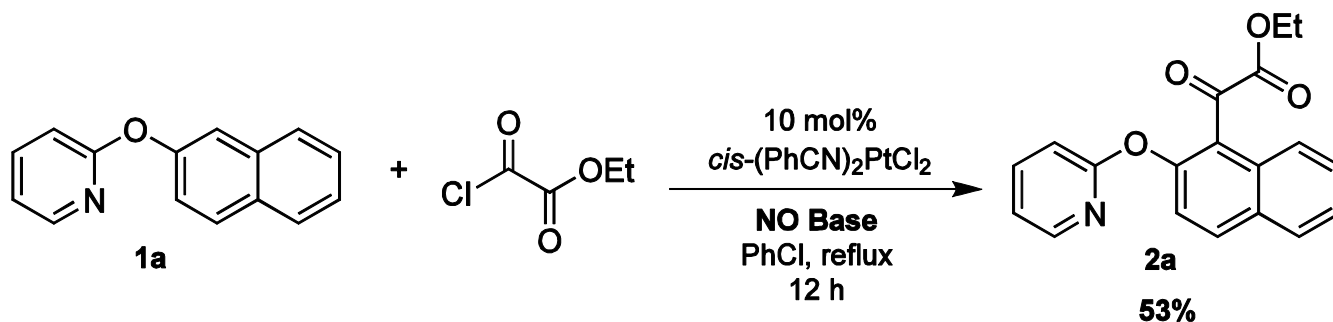
To further test this hypothesis, a reaction was done using the monoacylated product of the

2-(naphthalen-2-yloxy)pyridine (**1a**) which was then treated with 1eqivalent of HCl (from con.

hydrochloric acid). The reaction was refluxed under argon in chlorobenzene to mimic the

conditions the product would be at the completion of an acylation reaction. Mesitylene was used

as internal standard and was compared to the amount of product remaining at 0, 1, 3, and 12

hours. It was found at the conclusion of this experiment that no product degradation occurred

after 1h of reflux. However, after 3h. of reflux a 21% product loss was seen followed by a 38%

loss after 12h. Though it is not completely clear if the (PhCN)$_2$PtCl$_2$ is also playing a role in the

degradation of the product, these results help demonstrate the effectiveness of the K$_2$CO$_3$

addition to the overall reaction in its prevention of product degradation.

To further demonstrate the effectiveness the presence of K$_2$CO$_3$ has on the overall

reaction, an experiment was performed to determine how the presence of the base would impact

the reaction in the presence of 10% $(PhCN)_2PtCl_2$ (**Scheme 13**). The reaction was run under the

optimized base condition to determine if the product would degrade as seen in **Scheme 12** and to

determine if the catalyst was given ample time the yield could surpass the previously reported.

After the 12h reaction it was noted that the reaction mixture was dark orange, but no black

precipitates had formed in the reaction vessel. It is also important to note that the TLC plate

showed no starting material remained. Following workup, the overall reaction had a percent

yield of 87%. The resulting high yield can most likely be attributed to the presence of K_2CO_3 in

the reaction vessel.

Scheme 13 Pt- catalyzed ortho acylation reaction using 10% catalytic load and K_2CO_3
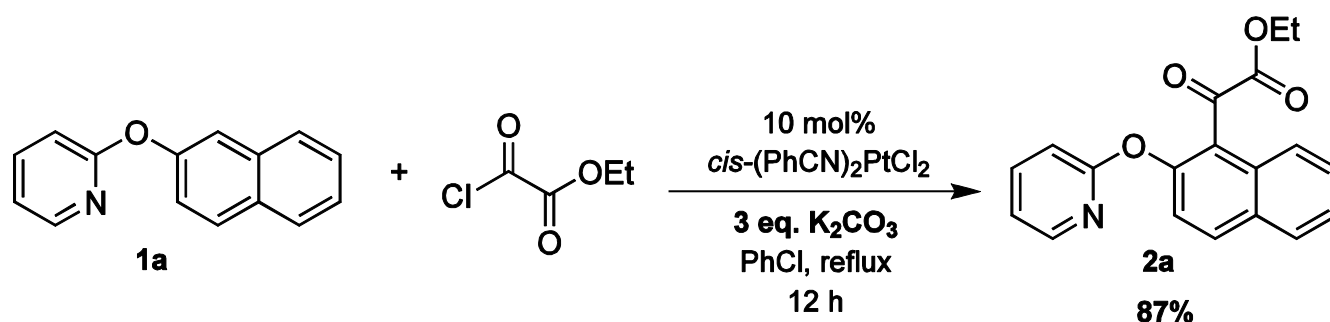
3.5 Experimental Section

All reactions involving moisture- and/or oxygen-sensitive compounds were carried out

under argon atmosphere and anhydrous conditions. All anhydrous solvents used were purchased

from Aldrich Chemical Co. with Sure Seal and used as received. The *cis*-Pt(PhCN)$_2$Cl$_2$, was

prepared according to literature procedures. Ethyl chlorooxoacetate was purchased from Sigma

Aldrich and was used as received. Thin layer chromatography was performed with silica gel 60

F254 plates, purchased from EMD chemicals. Gas chromatography was performed on a

Shimadzu GC-2010 AFC equipped with FID detector. [1]H spectra were recorded on a Bruker 400

MHz spectrometer at 298K using CDCl$_3$.

General Procedure for Base Optimized Pt-catalyzed acylation reaction

A 50 mL, three-necked round-bottom flask with a condenser was dried and charged with argon, and then charged with 2-(naphthalen-2-yloxy)pyridine (110.75 mg, 0.5 mmol), cis-$(PhCN)_2PtCl_2$ (11.95 mg, 0.025 mmol), ethyl chlorooxoacetate (0.17 ml, 1.5 mmol), K_2CO_3 (207.3mg, 1.5 mmol), tetradecane (32.5 µL) and anhydrous chlorobenzene (3 mL). The mixture was stirred and heated at reflux for 12 h. The temperature was lowered to 100 °C and quenched with pyridine (1.0 ml) which was added drop wise to the reaction mixture. After being stirred for 1 hour, the mixture was filtered through celite. The filtrate was transferred to a 250 ml separatory funnel, H_2O (20 ml) was added, and the aqueous layer was extracted with ethyl acetate (3 x 20 mL). The organic layers were combined and washed with $NaHCO_3$. The resulting solution was dried over $MgSO_4$, filtered, and concentrated via rotary evaporator. The product was isolated and purified via column chromatography on silica gel with hexanes-ethyl acetate (4:1) as the eluting solvent, yellow solid, 134.9 mg, 79.0%. The resulting solid was confirmed on ^{1}H NMR and compared with the previously reported spectra[34].

3.6 Summary of Findings

It was found at the conclusion of this investigation that HCl produced during the C-H activation step (**Scheme 8**) is playing a role in the catalytic loading for the acylation of 2-phenoxypyridines. This exploration has demonstrated that through the use of K_2CO_3 the catalytic requirements can be reduced from 10% to 5% essentially reducing the reaction cost by 50%. The lower catalytic requirements can be attributed to neutralization of the HCl. By neutralizing the acid, the platinum no longer must compete with HCl for binding to the substrate thus allowing for a more efficient catalytic cycle. Through application studies the reduced catalytic load was applied to various previously reported reactions. These experiments produced a marginal yield difference (5%-

15%) demonstrating how the 50% reduction in catalytic loading can still give comparable results. The K_2CO_3 addition also helped to give insight into product degradation pathways that had been previously seen. Neutralizing the HCl that is produced has helped eliminate the concern for product degradation. Future studies involving the reduction of catalytic loading could involve the further exploration of bases and the role they play in the acid neutralization, as well as the synthesis of novel hemilabile Pt(II) based catalysts that could potentially coordinate more effectively than the $(PhCN)_2PtCl_2$.

CHAPTER 4: EXPANSION OF ACYLATING REACTION SCOPE

4.1 Exploration of β and γ keto-ester acylating reagents

Following the novel synthesis involving the introduction of the α-keto ester functional

group through Pt-catalyzed direct C–H acylation[34] by the Huo group; it became necessary to

explore the diversity of this reaction through screening various keto ester acylating reagents.

Ethyl malonyl chloride and ethyl succinyl chloride were both explored to evaluate how the

addition of carbon linkers between the ketone and ester would affect its ability to participate in

the Pt-catalyzed acylation reaction.

The β-keto ester was the first of the two reagents to be explored. To test its reactivity the

ethyl malonyl chloride was allowed to react with 2-(naphthalen-2-yloxy)pyridine using 10%

(PhCN)$_2$PtCl$_2$ as catalyst (**Scheme 14**). The substrate and reaction condition were chosen due to

the favorable yield (76%) produced when the same conditions were used with the ethyl

chlorooxoacetate[34].

Scheme 14 Pt-Catalyzed C-H Acylation of **1a** with Ethyl Malonyl Chloride
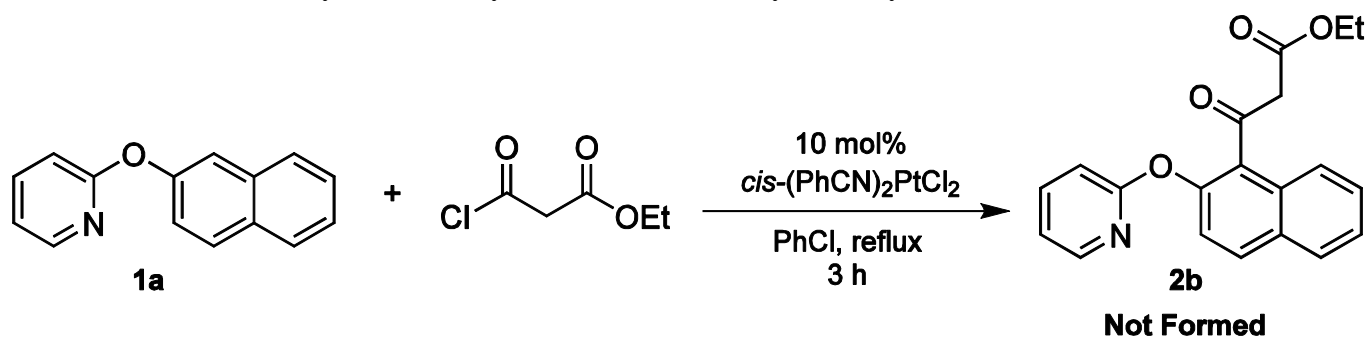
Following a 3 h reflux the solution turned a dark orange/black color, TLC showed no

reaction. This lack of reactivity can be attributed to a variety of different factors. First it is

possible that the acidic protons on the α carbon were deprotonated by the 2-phenoxypyridine

deactivating the β-keto ester to form a ketene and would no longer be able to undergo acylation. It is also possible that the ethyl malonyl chloride would react with the (PhCN)$_2$PtCl$_2$ catalyst inducing ligand exchange and forming a PtL$_2$ species that could no longer catalyze the reaction. The β-keto ester reaction was then tested using the base optimized method discussed in the previous chapter producing no reaction.

The γ-keto ester was the second of the reagents to be explored. It was hypothesized that through the addition of a second carbon spacer the problem experienced with the β-keto ester would be alleviated. By not having the two strong electron withdrawing groups so close the α and β protons would not be as acidic and would leave the reagent intact. To test its reactivity the ethyl succinyl chloride was reacted with 2-(naphthalen-2-yloxy)pyridine using 10% (PhCN)$_2$PtCl$_2$ as catalyst (**Scheme 15**).

Scheme 15 Pt-Catalyzed C-H Acylation of **1a** with Ethyl Succinyl Chloride
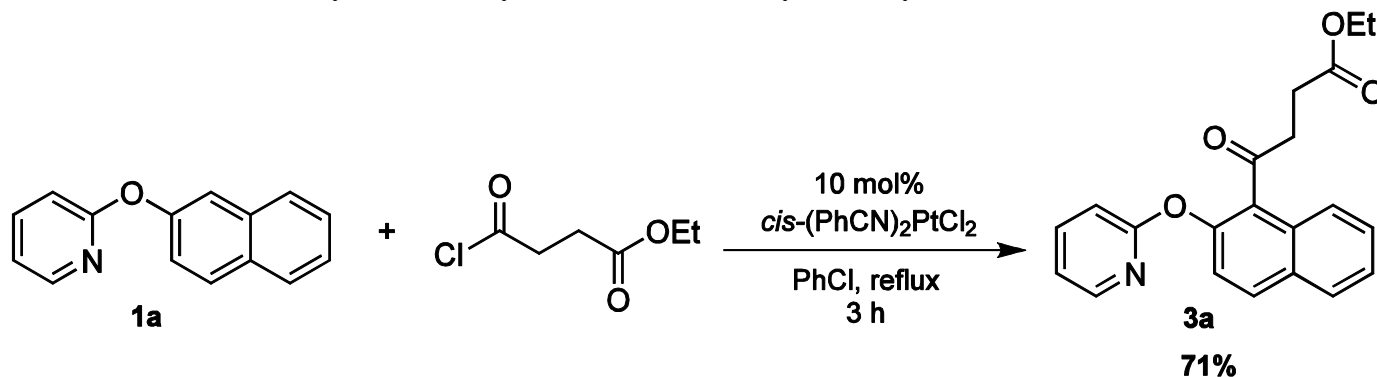
Following a 3h reflux a reaction was seen producing a yellow oil with a 79% yield with the product being confirmed via 1H NMR (See section below for further elucidation discussion). The success of this reaction identifies that the problems seen with the β-keto ester does not plague this reagent since the central protons are not as acidic. The base optimized lower catalytic load reaction conditions were applied to the γ-keto ester. No reaction was seen on TLC or GC

after 3 h of reflux. It is possible that though the α and β protons are not too acidic to be destroyed by the 2-(aryloxy)pyridine but are still slightly too acidic to be unaffected by the K_2CO_3. The scope of the γ -keto ester was then explored with various substituted 2-phenoxypyridines (see the next section for further details).

4.2 Expansion of Acylating reaction using γ keto-ester

To further examine the γ-keto ester reaction several 2-(aryloxy)pyridines were acylated. Substituents included both electron donating groups and electron withdrawing groups at the *ortho, meta,* and *para* position to examine how varying electronic effects would affect acylation. Mono and di- acylated products have been combined in **Table 3** due to limited reactivity seen with *para* substituted 2-aryloxypyridines.

The first of the 2-aryloxypyridines to be acylated was **1a,** forming **3a.** This reaction proceeded for 3 h and had a yield of 71%. This yield can be attributed to naphthalene's higher reactivity than benzene. Naphthalene is less aromatic and has a high resonance energy (72 Kcal/mol) which allows the ethyl succinyl chloride to bind more readily. It was found that *ortho* substituted 2-aryloxypyridines (**3b-3e)** were unaffected by the varying electronic substituents with all of them having similar percent yields (62-64%). To further test this lack of electronic effect *meta* substituents were then examined. The *m*-OMe substituted 2-aryloxypyridine (**3f**) was the first to be tested. After examining the reaction at 1 h intervals for 3 h it was found that no more product was formed between the 2 h and 3 h mark. After isolating the product, a 64% yield was obtained. This yield was comparable to the *ortho* substituted products, however the reaction finished earlier implying that electron donating groups made the 2-aryloxypyrine more reactive with the ethyl succinyl chloride. To further expand this theory *m*-Cl and *m*-NO₂ substituted 2-aryloxypyridines were reacted. After 3h it was found that a significant amount of starting

material remained when the TLC was performed. The product was isolated giving a 55% yield of the m-Cl product (**3g**). When the m-NO$_2$ substituted substrate was reacted it was found that no product was formed. These results indicate that electron withdrawing groups slow the reaction to a point where it may not even proceed. This could be due to the reduction of electron richness in the substrate making it a weaker nucleophile making it difficult for the already weaker electrophile to acylate. The *para* substituted 2-aryloxypyridines were then explored. Limited to no diacylated products were formed when the electron withdrawing groups were present. In the case of **3j** small amounts of potential product were seen on the TLC plate but the spot was so small it was not isolated further. In the case of **3k** no reaction was seen at all. These results indicate that the 2-aryloxypyridines are highly sensitive to electronic effects even more so at the *para* position than the *meta* position. This could be due to inductive effects experienced by the Pt-catalyst when it is bound to the ring making it a weaker nucleophile. However more mechanistic probing is needed to fully elucidate the underlying factors responsible for this drastic difference in reactivity at the *meta* and *para* positions.

Table 3 Pt-catalyzed synthesis of γ-keto ester with 2-aryloxypyridines

3a, 71%

3b, 62%

3c, 63%

3d, 62%

3e, 64%

3f, 64%

3g, 55%

3h, NR

3j (?) Trace

3k, NR
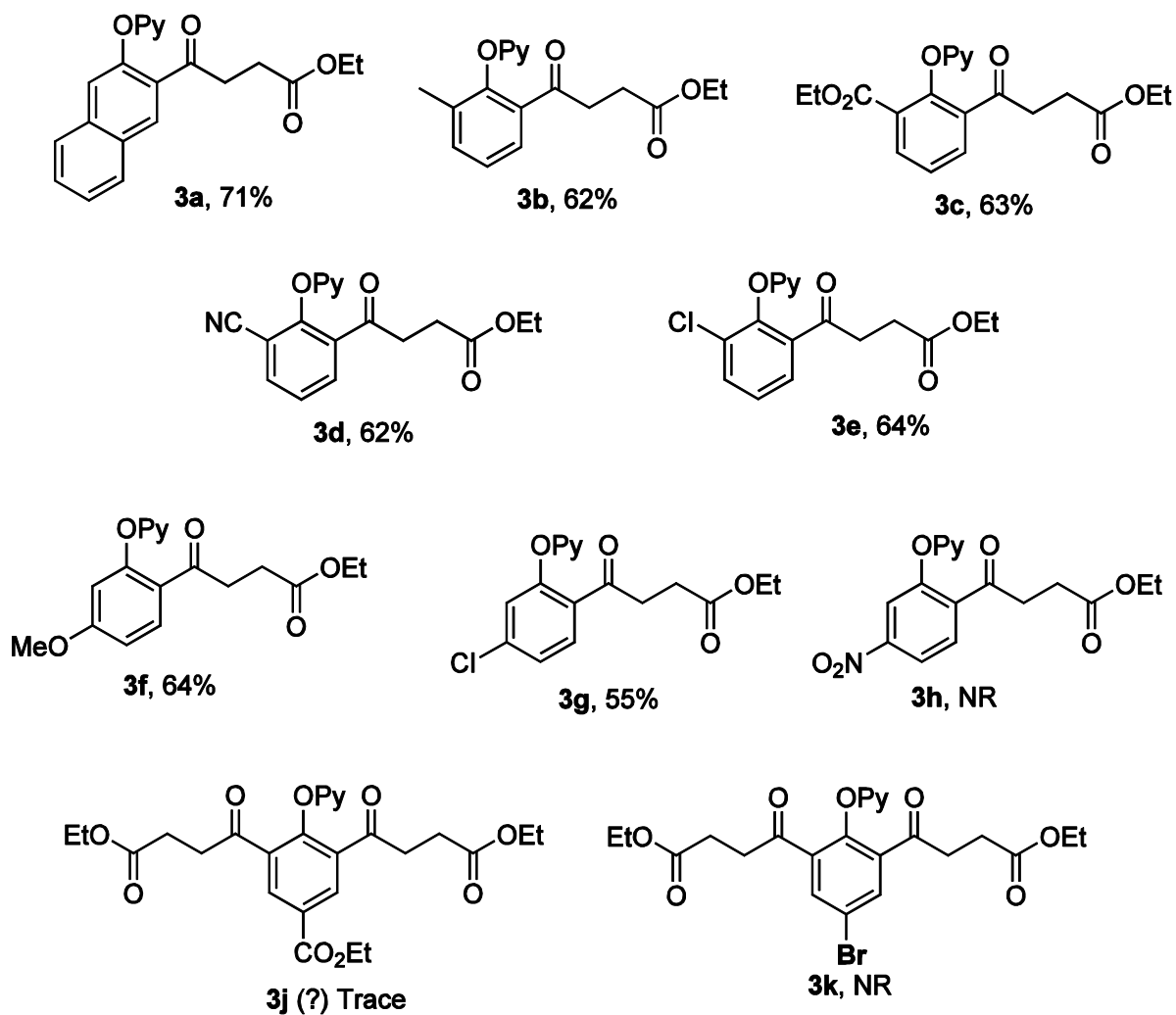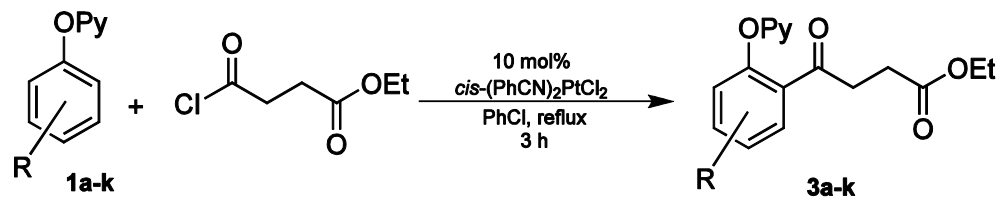
^a General conditions: 2-aryloxypyridine (0.5 mmol), ethyl succinyl chloride (1.5 mmol), *cis*-Pt(PhCN)$_2$Cl$_2$, chlorobenzene (3 mL), reflux. The reaction time was not optimized. Yields are isolated yields.

4.3 Competing Reaction Study

Scheme 16 Competing Acylation of **1b** with Ethyl Chlorooxoacetate and Ethyl Succinyl
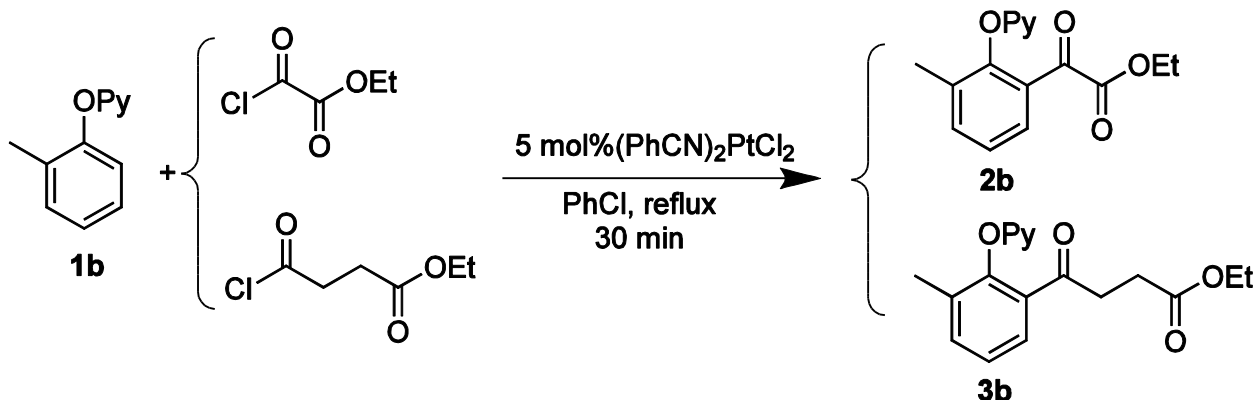
Chloride

A competing reaction was performed (**Scheme 16**) to compare relative reactivity of ethyl chlorooxoacetate and ethyl succinyl chloride. 2-(2-methylphenoxy)-pyridine was selected as the substrate due to the fact that the NMR signals of the products could be readily assigned for quantitative analysis. The reaction used 0.5 equivalents of both acylating reagents to cause a more direct competition for the site of acylation. The reaction was also stopped after 30 min to identify the selectivity of the two reagents during the initial conversion of the reaction. Previously performed experiments suggested that the α-keto ester would be the favored species due to the strength of the more electron-deficiency of ethyl chlorooxocetate compared to the ethyl succinyl chloride which has the two-carbon spacer separating the ester from the acyl chloride. The α-keto ester reactions were shown to have an average reflux time of 1h whereas the γ -keto ester saw an average of 3h, the difference in this synthetic time can most likely be attributed to the position of the ester group in both reagents. This difference was further demonstrated by the competing reaction. The difference in yield was identified by taking 1H NMR of the crude (**Figure 1**) and isolated (**Figure 2**) reaction mixtures and the resulting methyl

shifts (2.24-2.08 ppm) were then used to identify the product ratio. The combined product ratio was 8.9:1 of the α -keto ester to the γ -keto ester products which was consistent across both the crude and isolated spectra. This difference in reactivity suggests that having the two-electron withdrawing groups next to each other in the α-keto ester increases the overall electrophilicity of the reagent whereas the carbon spacers reduce electrophilint, consistent with the previously reported experiments.

Figure 1 ^{1}H NMR of crude reaction mixture from competing reaction of **1b** with **2c** and **3b**
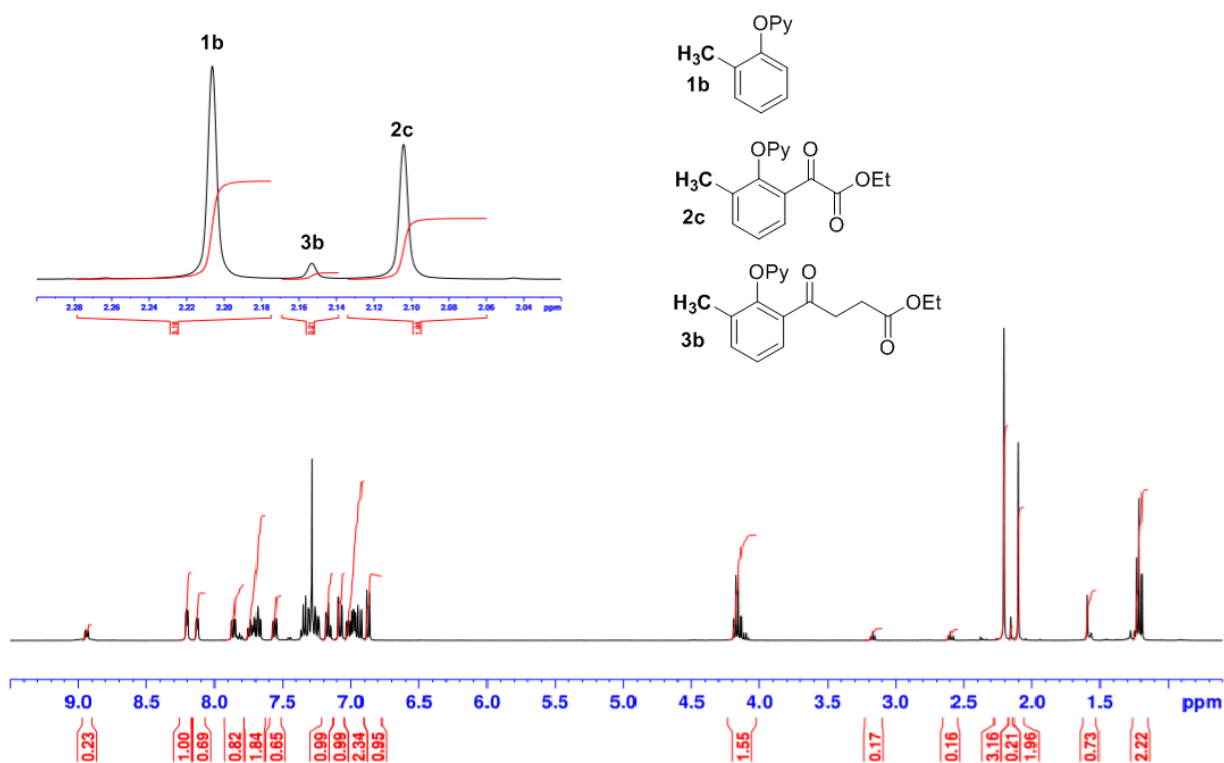
Figure 2 1H NMR of isolated reaction mixture from competing reaction of **1b** with **2c** and **3b**
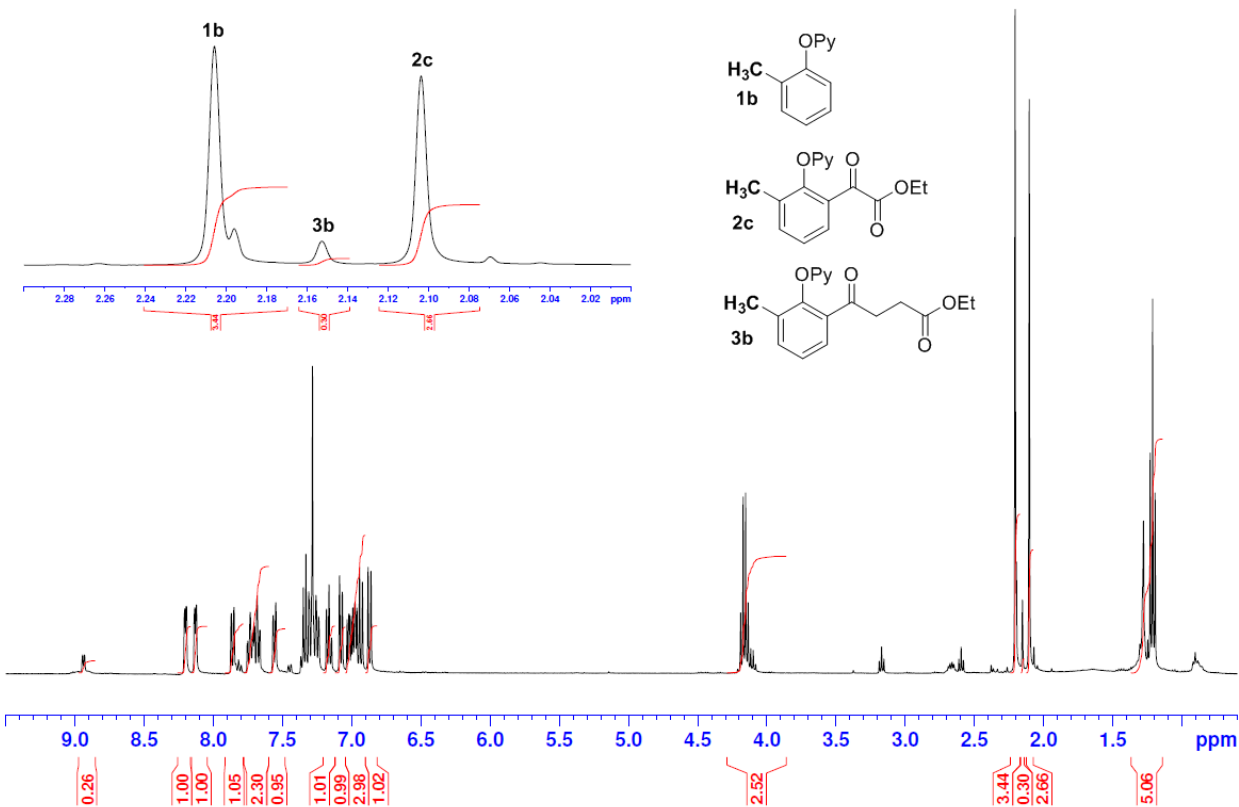
4.4 Experimental Section

All reactions involving moisture- and/or oxygen-sensitive compounds were carried out under argon atmosphere and anhydrous conditions. All anhydrous solvents used were purchased from Aldrich Chemical Co. with Sure Seal and used as received. *cis*-Pt(PhCN)$_2$Cl$_2$, and *trans*-Pt(PhCN)$_2$Cl$_2$, were prepared according to literature procedures. Ethyl succinyl chloride was purchased from Sigma Aldrich and was used as received. Thin layer chromatography was performed with silica gel 60 F254 plates, purchased from EMD chemicals. Gas chromatography was performed on a Shimadzu GC-2010 AFC equipped with FID detector. ^{1}H and ^{13}C NMR spectra were recorded on a Bruker 400 MHz spectrometer at 298K using CDCl$_3$. Chemical shifts were reported relative to TMS (0.0 ppm for 1H), chloroform-d (77.0 ppm for 13C) and coupling constants (J) were reported in Hertz. Mass spectra were measured on a Waters UPLC/Micromass

28

Quadrupole-ToF mass spectrometer. All ligands were prepared according to previously reported literature procedure.[34]

General Procedure for Acylation of 2-phenoxypyridine using gamma-keto esters

General Procedure A. Under argon a 50 mL, three-necked round-bottom flask with a condenser was dried, and then charged with 2-(naphthalen-2-yloxy)pyridine (110.75 mg, 0.5 mmol), *cis-*(PhCN)$_2$PtCl$_2$ (23.9 mg, 0.05 mmol), ethyl succinylchloride (0.29 ml, 1.5 mmol), tetradecane (32.5 µL) and anhydrous chlorobenzene (3 mL). The mixture was stirred and heated at reflux for 3 h. The temperature was lowered to 100 °C and quenched with pyridine (1.0 ml) which was added dropwise to the reaction mixture. After being stirred for 1 hour, the mixture was filtered through celite. The filtrate was transferred to a 250 ml separatory funnel, H$_2$O (20 ml) was added, and the aqueous layer was extracted with ethyl acetate (3 x 20 mL). The organic layers were combined and washed with NaHCO$_3$. The resulting solution was dried over MgSO$_4$, filtered, and concentrated via rotary evaporator. The product was isolated and purified via column chromatography on silica gel with hexanes-ethyl acetate (3:1) as the eluting solvent, yellow solid, 124.0 mg, 71.0%.

The following compounds were synthesized using General Procedure A.
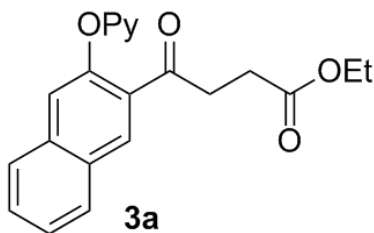
Synthesis of 3a. Purified via column chromatography on silica gel with hexanes-ethyl acetate (v/v = 3:1): yellow solid, 76.4% yield. Melting point: 76-77.0 °C. **NMR** (400 MHz, CDCl$_3$): δ

8.40 (s, 1H), 8.18 (d, J=3.8 1H), 7.97 (d, J=8.2 1H), 7.86-7.73 (m, 2H), 7.65-7.46 (m, 3H), 7.05 (m, 2H), 4.14 (q, J=7.2 Hz, 2H), 3.35 (t, J = 6.7 Hz, 2H), 2.67 (t, J = 6.7 Hz, 2H), 1.25 (t, J = 7.1 Hz, 3H). **^{13}C NMR** (100 MHz, CDCl$_3$) δ 199.2, 172.8, 163.5, 149.1, 147.7, 139.8, 135.7, 131.6, 131.4, 130.3, 129.2, 128.4, 127.1, 126.1, 119.6, 118.9, 111.8, 60.6, 37.3, 28.6, 14.2. **MS** Calculated for C$_{21}$H$_{19}$NO$_4$ (M+H$^+$) 350.13; Found: 350.14.

3b
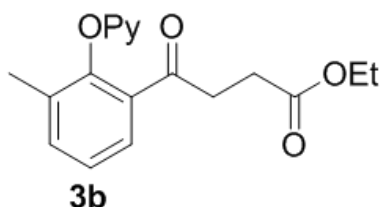
Synthesis of 3b. Purified via column chromatography on silica gel with hexanes-ethyl acetate (v/v = 3:1): yellow oil, 64% yield. **^{1}H NMR** (400 MHz, CDCl$_3$): δ 8.13 (m, 1H), 7.76-7.65 (m, 2H), 7.45 (m, 1H), 7.25 (d, J=7.7 Hz, 1H), 7.01-6.91 (m, 2H), 6.60 (d, J=2.4 Hz, 1H), 4.11 (q, J=7.1 Hz, 2H), 3.17 (t, J = 6.7 Hz, 2H), 2.60 (t, J = 6.7 Hz, 2H), 2.15 (s, 3H) 1.23 (t, J = 7.1 Hz, 3H). **^{13}C NMR** (100 MHz, CDCl$_3$) δ 199.5, 172.8, 163.0, 150.0, 147.7, 139.7, 135.1, 132.7, 132.6, 127.6, 125.5, 118.3, 110.6, 60.5, 37.3, 28.6, 16.7, 14.2. **MS** Calculated for C$_{18}$H$_{19}$NO$_4$ (M+H$^+$) 315.13; Found: 315.14.

3c

Synthesis of 3c. Purified via column chromatography on silica gel with hexanes-ethyl acetate (v/v = 3:1): yellow oil, 64% yield. **^{1}H NMR** (400 MHz, CDCl3): δ 8.12 (dd, J=7.7, 1.8 Hz, 1H), 8.05 (m, 1H), 7.98 (dd, J=7.8,1.8 Hz, 1H), 7.79-7.70 (m, 1H), 7.39 (t, J=7.7 Hz, 1H), 7.05 (d, J=8.3 Hz, 1H), 7.00-6.94 (m, 1H) 4.10 (qd, J=7.1, 1.2 Hz, 4H), 3.17 (t, J = 6.6 Hz, 2H), 2.62 (t, J = 6.6

Hz, 2H), 1.22 (t, J = 7.1 Hz, 3H), 1.08 (t, J = 7.1 Hz, 3H). **^{13}C NMR** (100 MHz, CDCl$_3$) δ 199.3, 172.6, 165.0, 163.3, 15.7, 147.2, 139.7, 135.1, 134.2, 133.8, 126.3, 125.3, 118.5, 111.1, 61.2, 60.6, 37.9, 28.6, 14.2, 13.9. **MS** Calculated for C$_{20}$H$_{12}$NO$_6$ (M+H$^+$) 372.14; Found: 372.14.

3d

Synthesis of 3d. Purified via column chromatography on silica gel with hexanes-ethyl acetate (v/v = 3:1): yellow oil, 62% yield. **^{1}H NMR** (400 MHz, CDCl$_3$): δ 8.22 (m, 1H), 7.86 (d, J = 8.5 Hz, 1H), 7.83-7.75 (m, 1H), 7.26 (d, J=1.8 Hz 1H), 7.15 (d, J=1.8 Hz, 1H), 7.12-7.09 (m, 1H), 7.07-7.05 (d, J=8.3 Hz, 1H) 4.13 (q, J=7.1 Hz, 2H), 3.24 (t, J = 6.6 Hz, 2H), 2.65 (t, J = 6.6 Hz, 2H), 1.24 (t, J = 7.1 Hz, 3H). **^{13}C NMR** (100 MHz, CDCl$_3$) δ197.8, 172.7, 162.4, 153.6, 147.9, 140.1, 138.9, 131.4, 129.5, 125.3, 122.9, 119.6, 112.2, 60.6, 37.7, 28.5, 14.2. **MS** Calculated for C$_{18}$H$_{16}$N$_2$O$_4$ (M+H$^+$) 325.11; Found: 325.12.
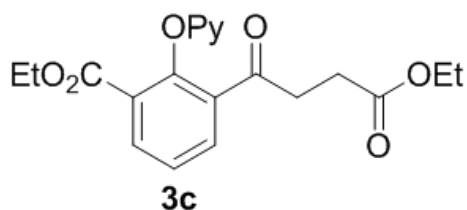

3e

Synthesis of 3e Purified via column chromatography on silica gel with hexanes-ethyl acetate (v/v = 3:1): yellow oil, 64% yield. **^{1}H NMR** (400 MHz, CDCl$_3$): δ 8.11 (m, 1H), 7.81-7.73 (m, 2H), 7.63 (dd, J=7.9, 1.7 Hz, 1H), 7.31 (d, J=7.9 Hz, 1H), 7.10-7.01 (m, 2H), 6.60 (d, J=2.4 Hz, 1H), 4.11 (q, J=7.1 Hz, 2H), 3.17 (t, J = 6.6 Hz, 2H), 2.62 (t, J = 6.6 Hz, 2H), 1.23 (t, J = 7.1 Hz, 3H). **^{13}C NMR** (100 MHz, CDCl$_3$) δ 198.3, 172.6, 162.4, 148.2, 147.5, 139.8, 134.5, 134.0, 129.3,

128.4, 126.2, 118.9, 111.0, 60.6, 37.4, 28.5, 14.2MS Calculated for $C_{17}H_{16}ClNO_4$ (M+H$^+$)

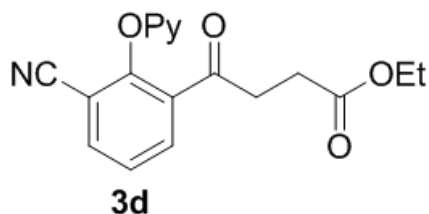334.08, 336.07; Found: 322.

3f

Synthesis of 3f. Purified via column chromatography on silica gel with hexanes-ethyl acetate (v/v

= 3:1): yellow oil, 64% yield. **^{1}H NMR** (400 MHz, CDCl$_3$): δ 8.22 (m, 1H), 7.96 (d, J = 8.84 Hz,

1H), 7.80-7.72 (m, 1H), 7.12-6.98 (m, 2H), 6.82 (dd, J=11.4, 6.4 Hz, 1H), 6.60 (d, J=2.4 Hz,

1H), 4.11 (q, J=7.1 Hz, 2H), 3.8 (s, 3H), 3.23 (t, J = 6.7 Hz, 2H), 2.62 (t, J = 6.7 Hz, 2H), 1.23 (t,

J = 7.1 Hz, 3H). **^{13}C NMR** (100 MHz, CDCl$_3$) δ 196.9, 173.0, 163.9, 162.9, 155.1, 148.0, 139.8,

132.3, 123.7, 119.1, 112.0, 111.0, 107.8, 60.5, 55.6, 37.4, 28.7, 14.2 **MS** Calculated for

$C_{18}H_{19}NO_5$ (M+H$^+$) 330.13; Found: 330.13.
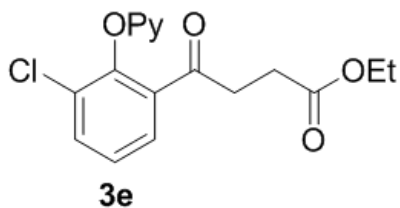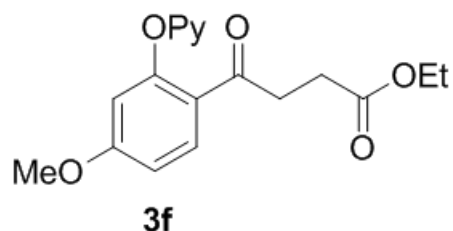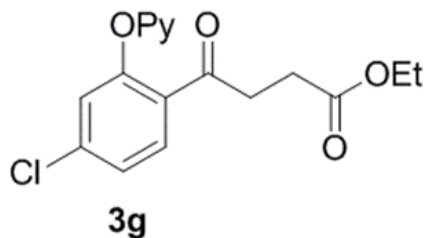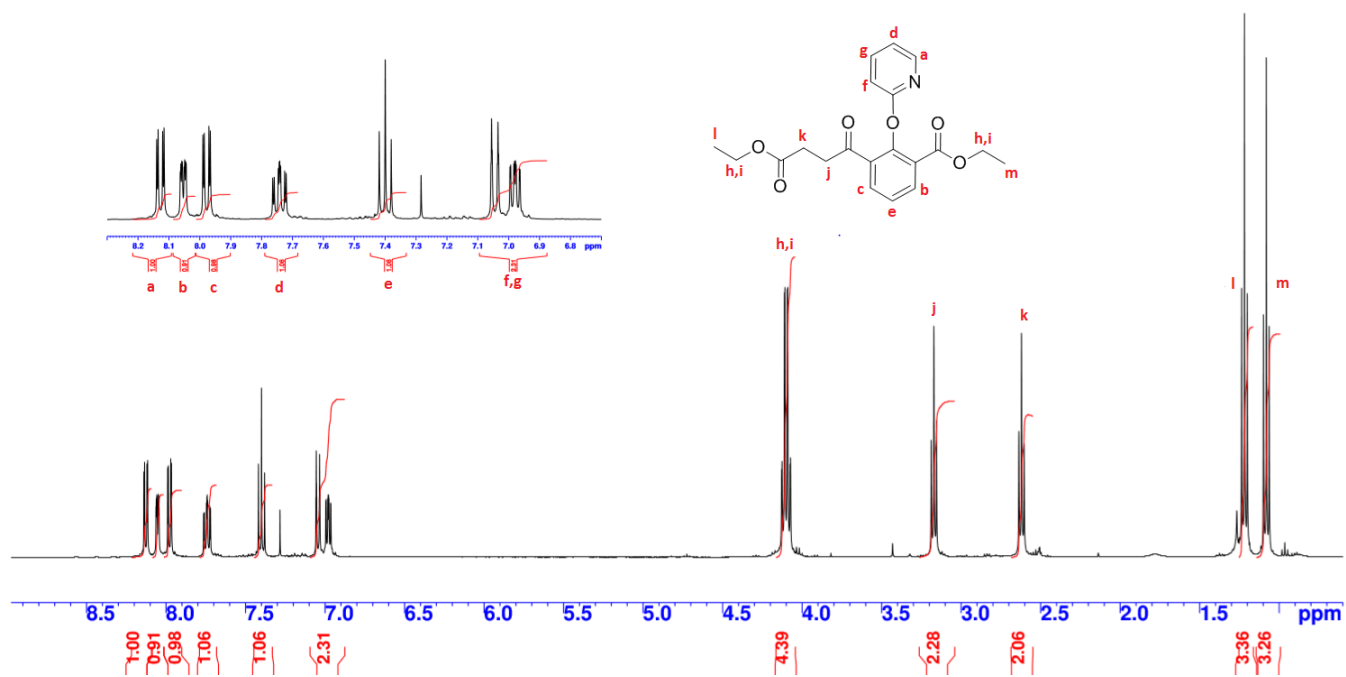

3g

Synthesis of 3g. Purified via column chromatography on silica gel with hexanes-ethyl acetate

(v/v = 3:1): yellow oil, 64% yield. **^{1}H NMR** (400 MHz, CDCl$_3$): δ 8.22 (m, 1H), 7.86 (d, J = 8.5

Hz, 1H), 7.82-7.76 (m, 1H), 7.26 (d, J=2.0, 1H), 7.15 (d, J=1.9 Hz, 1H), 7.13-7.04 (m, 2H), 4.13

Figure 3 Assigned 1H NMR spectra of **3c**

CHAPTER 5: MECHANISTIC INSIGHT INTO SUBSTITUENT EFFECTS

5.1 The role of substituents in the acylation of 2-phenoxypyridines

Following the discovery of the Pt-catalyzed acylation reaction it was noted that varying

the substituents on the 2-phenoxypyridine appeared to affect the rate of the reaction. During the

initial study benzoyl chloride was used to acylate various 2-phenoxypyridines[4]. When electron-

withdrawing groups were present at the *meta* and *para* position regarding the metalated carbon a

decrease in reactivity was noted. With the presence of and electron-donating group however, the

rate of reaction was increased with high yields in a shorter period of time. The study that

followed used ethyl cholorooxoacetate as acylating agent to introduce an α-keto ester to the 2-

phenoxypyridine[34]. During this study *ortho*, *meta*, and *para*-substituted 2-phenoxypyridines were

acylated. It was found that both electron-donating and electron-withdrawing groups are tolerated

producing comparable yields when ortho-substituted 2-aryloxypyridines were used. However, in

the *meta* position electron-withdrawing groups slowed the reactions with very strong electron-

withdrawing groups such as NO_2 resulting in no reaction at all. Similar results were observed

when exploring the diacylation of para-substituted substrates under the same reaction conditions.

When considering these experiments *ortho* position substituents do not affect the reaction no

matter the electronic nature of the group. However, the *meta* and *para* position see a large impact

based on the presence of various electronic groups. It is hypothesized that *ortho*-substituents do

not exert a large electronic effect. This is most likely due to the lack of resonance that occurs at

this site which ultimately prevents an effective electronic effect. It is also possible that the *meta*

and *para* positions may affect the formal electrophilic addition step mentioned in the proposed

mechanism. If electron withdrawing groups pull charge density away from the ring it could cause

a reduction in the overall rate of reaction due to the weakening of the of the nucleophile. In this chapter, a detailed study of the substituent effect by Hammett analysis will be described.

5.2 Experimental Design

To effectively examine substituent effects, competition experiments were utilized to determine the relative rate constants of the reactions of different substrates. Some advantages of performing such experiments include limiting error in heating that can occur when performing individual reactions since two substrates are in the same vessel; gaining the ability to examine how various substrates are able to directly compete for reagents gaining insight into selectivity; and reduction of overall time taken to perform experiments. When performing competing reactions some substrates are harder to identify due to similarity of structure, also when performing competing reactions identifying individual reaction rates can be found easier since the conversion can follow its normal pathway without other substrates present. Several experiments were performed to determine what would be the optimal reaction conditions to determine the relative rate constants. The initial experiments used the standard catalytic load of 10% $(PhCN)_2PtCl_2$ and the normal 1.5 equivalents of the acylating reagent. HPLC coupled with a UV-Vis detector was utilized but was soon replaced with ^{1}H NMR due to the shorter analysis time provided by the ^{1}H NMR and the ability to distinguish the starting material and products. The catalytic loading and acylating agent were eventually lowered in order to properly allow for the reaction to proceed at a slower rate so the sampling of the reaction at different intervals could be done conveniently.

Competition experiments comprised mostly of a standard unsubstituted 2-phenoxypyridine or 2-(3-methylphenoxy)-pyridine competing against another 2-aryloxypyridine that had been substituted with either an electron donating or electron withdrawing group

(**Scheme 9**). Samples were taken out of the reaction vessel at 0, 5, 10, 15, 20, 40, and 60 minutes

to identify early product conversion for accurate assessment of relative reaction rate constants.

The resulting sample ^{1}H NMR spectra were then compared with the previously reported

substrate and product spectra to identify the signals from starting materials and/or products that

could be monitored and used for calculation of conversion.

The calculated conversions were then plugged into the Ingold-Shaw expression

(**Equation 1**) where $[1x_0]$ and $[1y_0]$ represents the initial concentrations of the two substrates.

$[1x]$ and $[1y]$ represent the concentrations of the remaining starting material as the reaction

proceeds. When taking the logarithmic ratio, a linear relationship is produced which then

represents the competing rate constant. By doing this form of analysis a variety of substrates can

be tested at a much faster rate and be standardized across the varying experiments. Past

experiments have applied the Ingold-Shaw expression to accomplish a similar objective due to

its ability to test differing substrates ability to compete thus allowing for further insight into the

reaction kinetics[36].

Equation 1 Ingold Shaw Expression

$$\frac{k_x}{k_y} = \frac{\log\left(\frac{[1x]}{[1x_0]}\right)}{\log\left(\frac{[1y]}{[1y_0]}\right)}$$

5.3 Hammett Analysis

To determine how the various substituents affect the acylation reaction a linear free

energy relationship needs to be established. Hammett analysis was performed to determine the

overall sensitivity our reaction has to various substituents and potentially gain insight into charge

stability experienced throughout the reaction mechanism. Values derived from the competing

experiments where then plugged into the Hammett equation (**Equation 2)** where k represents the

rate constant for the various substituents and k_0 represents the rate constant for an unsubstituted

substrate. The symbol σ represents the substituent constant derived from Hammett's original

experiments and represents a specific substituent (ex. CO_2Et, Me, OMe etc.) and ρ represents the

reaction constant which gives insight into charge stability and the specific effect the various

substituents have. The ρ value can only be derived when the logarithmic ratio is plotted against

the σ. The resulting curve with the best correlation represents the linear free energy relationship

for the respective aromatic substituent.

Equation 2 Hammett Expression

$$\log \frac{K}{K_0} = \sigma\rho$$

Meta **Substituents**

The substituent effect at the *meta* position was the first to be explored. A competing

reaction was performed with 2-(3-methylphenoxy)-pyridine as the standard substrate instead of

an unsubstituted 2-phenoxypyridine (**Scheme 17**). The reason for this switch is that when the

ortho and *meta* positions lack a substituent, the reaction forms a diacylated product. The m-CH_3

was selected as standard since it has a relatively small electronic effect close to the m-H of the

unsubstituted 2-phenoxypyridine. Because of this change in standard the resulting Hammett plots

will have a shifted y-intercept. However, this does not affect the overall slope of the plot thus

charge sensitivity can still be derived.

Scheme 17 Competing reaction for *m*-Substituted 2-phenoxyopyridines
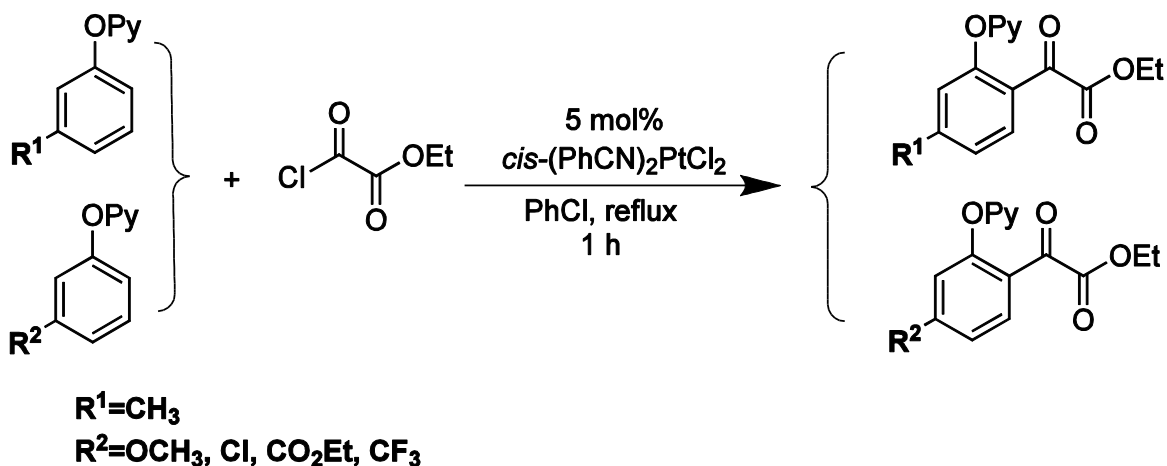
$R^1 = CH_3$
$R^2 = OCH_3, Cl, CO_2Et, CF_3$

Following the completion of the competing reaction ^{1}H NMR was performed on each of the sample pulls. **Figure 4** represents the full spectra for m-CH$_3$ vs. *m*-OCH$_3$ and **Figure 5** is the expanded version to demonstrate compound identification of the sample withdrawn at 20 min of reaction. The resulting peaks were equalized to 0.5 mmol (assuming the starting material only converted to the desired product because the reactions were clean) and the resulting ratios were plugged into the Ingold-Shaw expression with the resulting value found in **Table 4**.

Figure 4 1H NMR of crude reaction mixture at 20 min from competing reaction of *m*-CH$_3$ vs. *m*-OCH$_3$
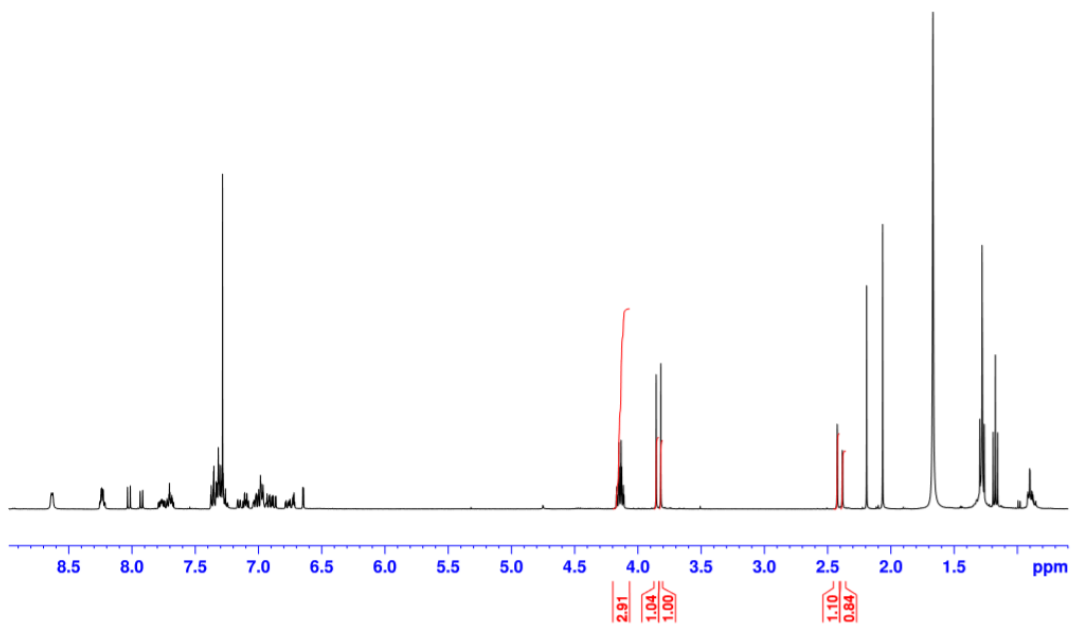
Figure 5 Expanded 1H NMR of crude reaction mixture at 20 min from competing reaction of *m*-CH₃ vs. *m*-OCH₃
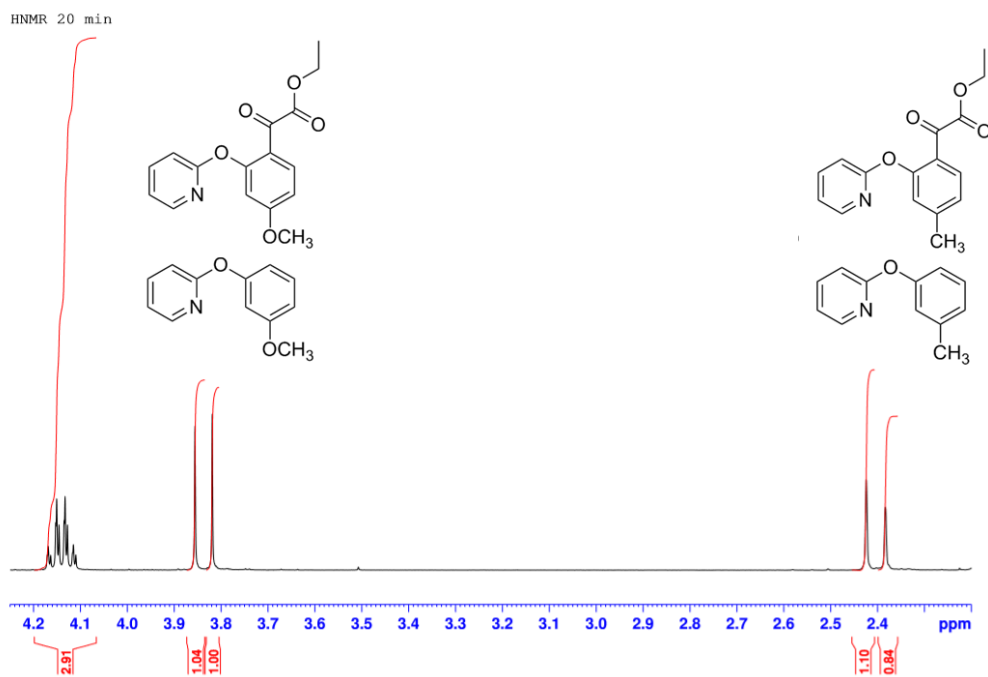
In some cases, it was difficult to discern substrate shifts aside from the m-CH$_3$ standard thus a different technique had to be applied to determine the amount of the substrate of interest remaining. In experiments where this was a prominent issue, the CH$_2$ signals from the α-keto esters were integrated to determine how much of both products had been formed. A ratio was then used to eliminate the amount of m-CH$_3$ present in this shift with the remainder being attributed to the competing product. This remainder was then subtracted by the initial concentration of 0.5 mmol and the amount substrate remaining could be calculated. **Figure 6** represents the full m-CH$_3$ vs. m-CF$_3$ spectra and **Figure 7** is the expanded version. To further validate the ratio method previously mentioned peaks associated with the m-CF$_3$ substrate and the product were found in the aromatic region of the spectra and used for the calculation of the relative rate constants. The resulting Ingold-Shaw values produced a difference of 0.4 (9.3% difference) this difference can be attributed to the ability to integrate cleanly in the aromatic region without picking up overlapping shifts.

Figure 6 1H NMR of crude reaction mixture at 20 min from competing reaction of *m*-CH₃ vs. *m*-CF₃
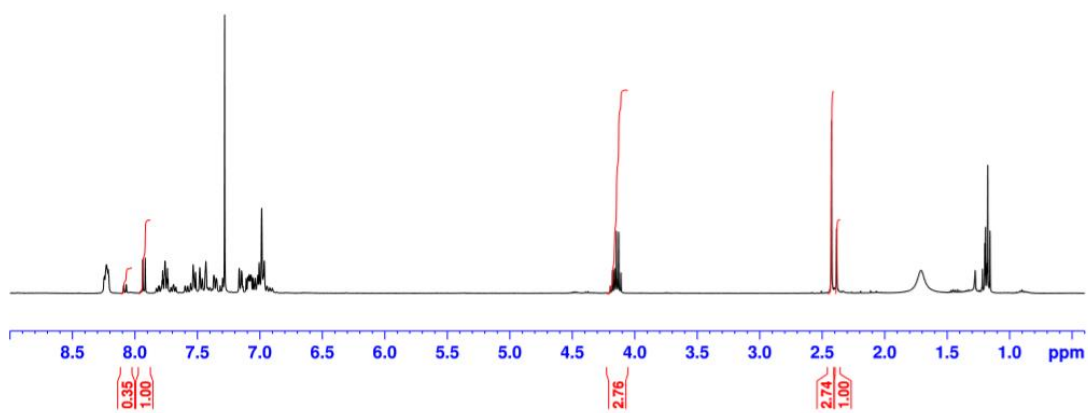
Figure 7 Expanded 1H NMR of crude reaction mixture at 20 min from competing reaction of *m*-CH₃ vs. *m*-CF₃
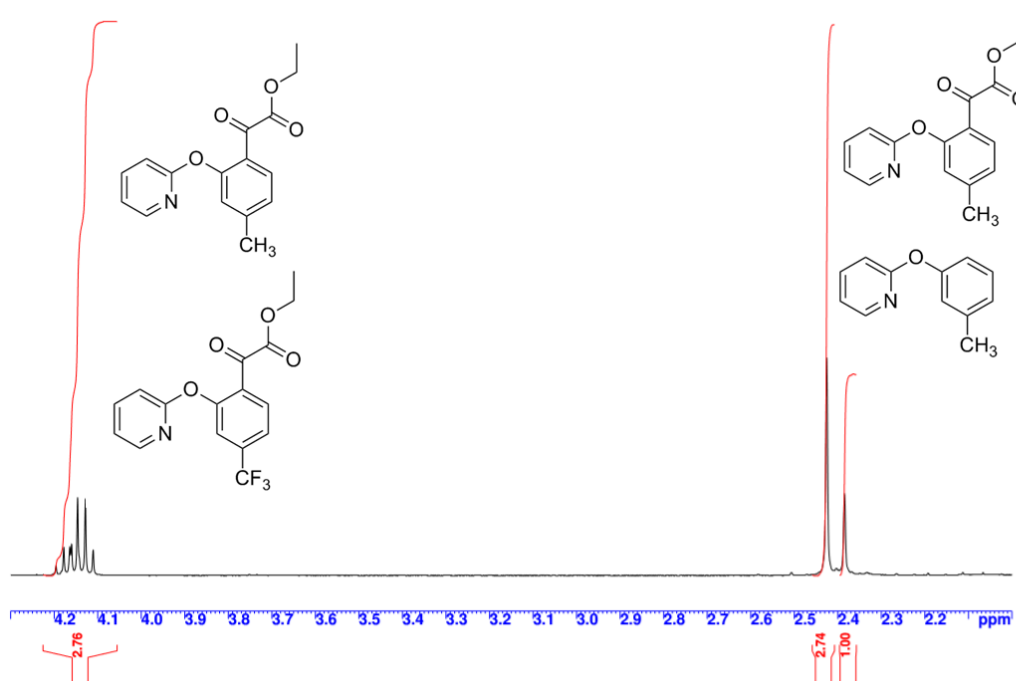
Table 4 Ingold-Shaw relative rate constants from the competition reactions of various *m*-substrates vs. a *m*-CH₃ standard

Substituent	CH₃
OMe	0.87 ±0.050
Cl	0.72 ±0.005
CO₂Et	0.35 ±0.025
CH₃	1.00 ±0.000
CF₃	0.45 ±0.064

[a] General conditions 2-(3-methylphenoxy)-pyridine (0.5 mmol), Substituted 2-aryloxypyridine (0.5 mmol), ethyl chlorooxoacetate (1.0 mmol), *cis*-Pt(PhCN)₂Cl₂ (0.05 mmol) chlorobenzene (6 mL), reflux, samples taken at 0, 5, 10, 15, 20, 40, and 60 min.

Following the Ingold-Shaw analysis the resulting rate constants were plugged into the Hammett equation producing the values found in **Table 5** (Log k/k_{CH3}). The Hammett values were then plotted against their standard sigma values[30]

Table 5 *m*-Hammett values for substituted 2-(aryloxy)pyridines

Substituent	Sigma m	Sigma p	Sigma +	Sigma -	Log(k/k_{CH3})
CH₃	-0.06	-0.14	-0.31	-0.17	0.000
Cl	0.37	0.24	0.11	0.19	-0.144
CO₂Et	0.36	0.48	0.49	0.75	-0.461
OMe	0.1	-0.27	-0.78	-0.26	-0.060
CF₃	0.43	0.54	0.61	0.65	-0.342

The first Hammett Plot explored was σ_{meta} (**Figure 8**). This plot primarily aimed to examine how *m*-substituents affect the overall reaction. Normally substituents with stronger inductive effects have more influence at this position than resonance effects when considering

42

charge stability. The linearity (0.6373) is poor. However, the negative sign of the slope demonstrates that the reaction rate was decreased by electron-withdrawing groups which agrees with the proposed mechanism and previously reported results[4, 34]. When considering the reaction mechanism mentioned in previous chapters (**Scheme 8**) the positive charge build up does not occur until the cyclometallation of the Pt(II) species with the 2-phenoxypyridine thus it is possible that the cyclometalated carbon is playing a role in charge stability due to its sharing electrons with the Pt(II). If this is the case the *m*-substituents must now be considered as *p*-substituents thus σ_{Para} needed to be explored.

Figure 8 σ_{meta} Hammett Plot for *m*-substituted 2-phenoxypyridines
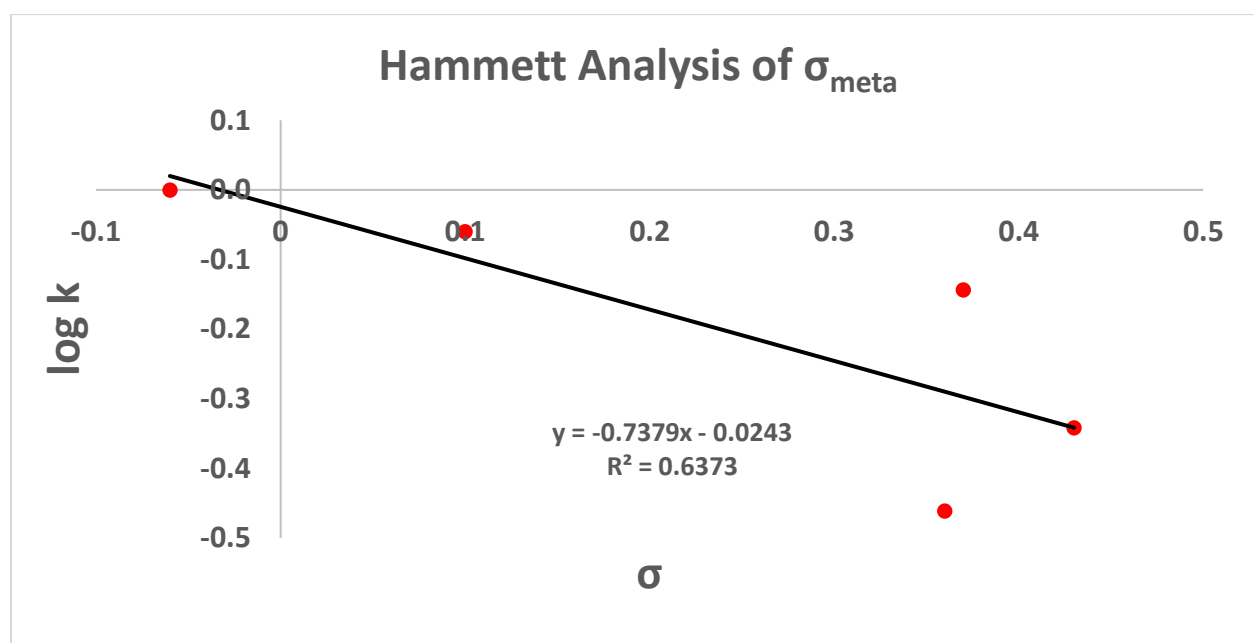
The second Hammett Plot explored was σ_{Para} (**Figure 9**). This plot aimed to determine if the resonance substituent effect is significant. The resulting Hammett plot produced significantly better linearity (0.8033) than that when plotting the σ_{meta} demonstrating that substituents with more resonance effect potential effect the overall charge stability and rate of reaction. The slope

for this plot remained negative demonstrating that there may be positive charge build up at the reaction center (ρ = -0.4799). Based on the better results seen when plotting regarding *p*-substituents further probing was needed to elucidate if electron-donating or electron-withdrawing provided a more significant impact on the overall reaction rate. With this in mind plots against σ^+ and σ^- need to be evaluated.

Figure 9 σ_{Para} Hammett Plot for *m*-substituted 2-phenoxypyridines
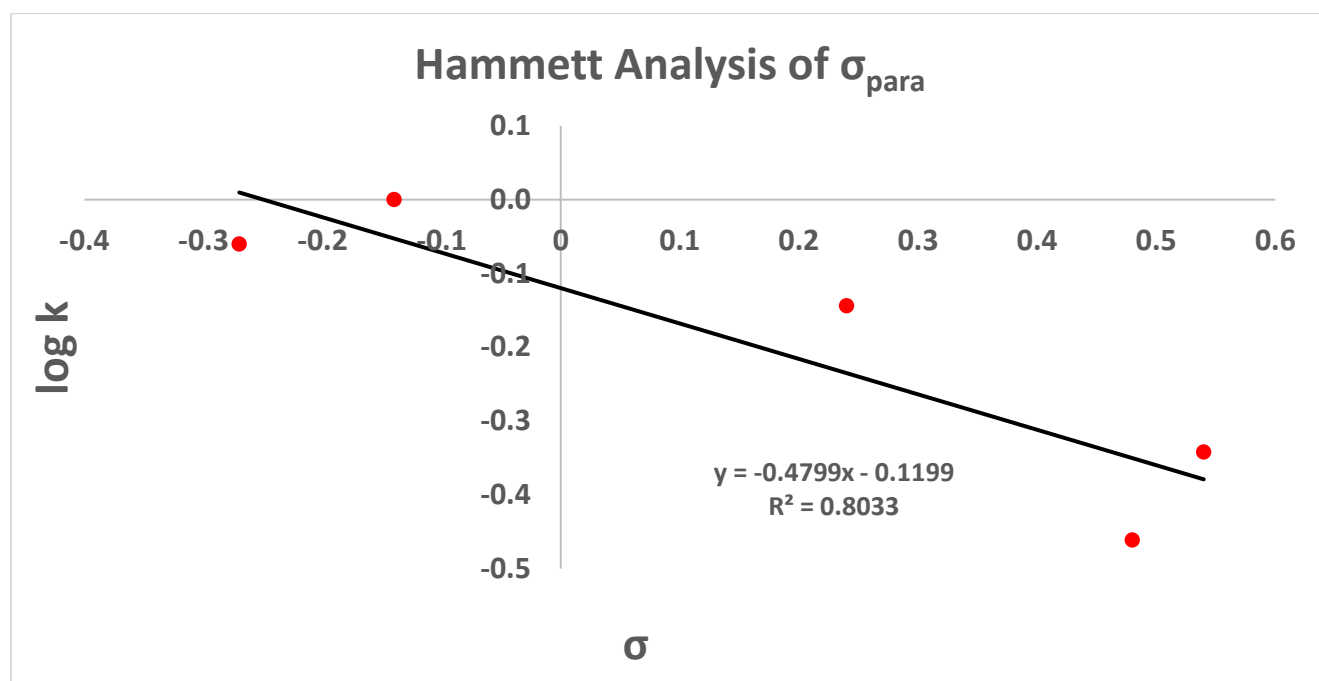
The third Hammett Plot explored was σ^+ (**Figure 10**). This plot aimed to examine how electron donating groups effect the overall charge stability due to resonance effects that are not appropriately measured via standard σ_{para} Hammett values when the reaction center is positively charged and there is direct resonance interaction with an electron-donating group. However, the poor correlation (0.718) does not suggest this scenario. The sensitivity for this plot is also low (ρ = -0.2862). However, it is also important to note that the plot provided only includes 2 groups

that can be considered electron donating groups (CH_3 and OCH_3) because stronger electron

donating groups (NR_2, and NH_2) prohibited the reaction.

Figure 10 σ_+ Hammett Plot for *m*-substituted 2-phenoxypyridines
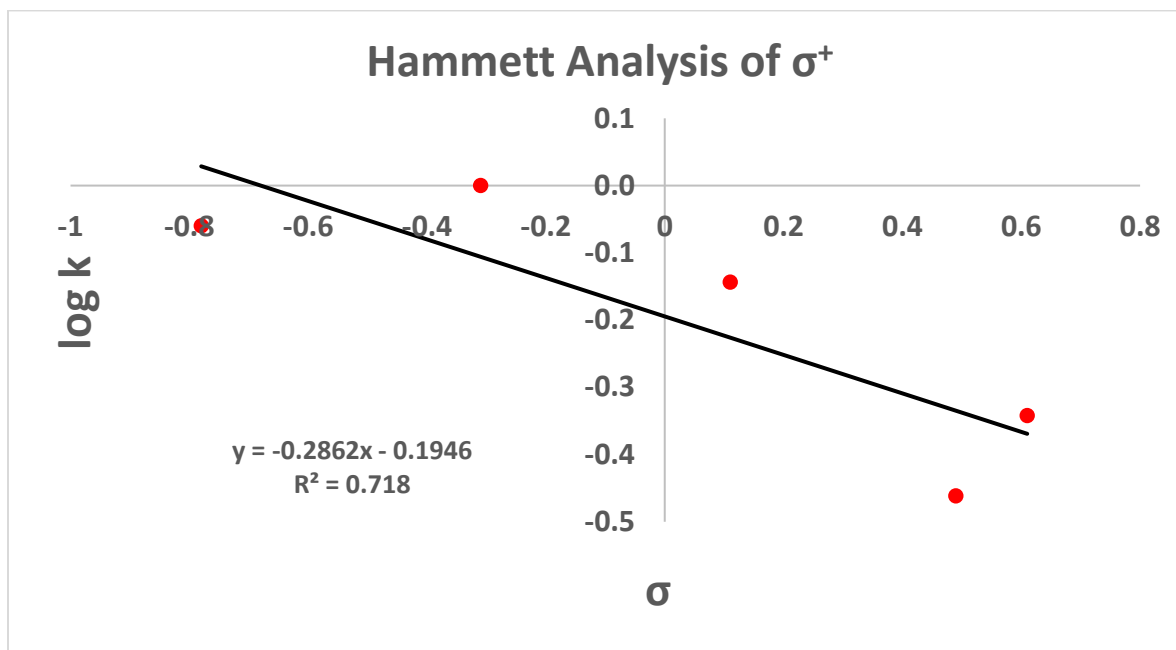
The fourth Hammett Plot explored was σ^- (**Figure 11**). Much like the previously

mentioned plot σ^- aims to help correlate enhanced resonance effect of strong electron-

withdrawing groups that fall outside of normal Hammett trends. The resulting correlation

(0.9349) was the best of the four plots and represents an acceptable correlation for Hammett

Analysis. The plot also demonstrates sensitivity to the substituents ($\rho = -0.4082$). This

correlation demonstrates that the reaction is affected heavily by the resonance effect of electron-

withdrawing groups. The resonance effect these substituents induced on the ring causes a

reduction in the rate of the reaction. This reduction in rate could be due to the pulling of electron

richness away from the ring making it more difficult for the formal electrophilic addition to

occur. The reduction of electron richness would make it so the substituted 2-phenoxypyridine

would be weaker nucleophile thus reducing the rate the acylating agent would react with the substrate. This result agrees with the previously reported slowing of reaction rate when electron-withdrawing groups are present on the 2-phenoxypyridine. It is also demonstrated through the negative log k/k_{CH3} value (**Table 5**) that the OCH_3 (-0.060) is experiencing a slight inductive effect during this reaction essentially acting as a very weak electron withdrawing group due to the electronegativity of the oxygen. This explains why the OCH_3 reaction proceeded at a slightly slower rate that the CH_3 standard. Since the CH_3 can only donate electrons into the ring where the OCH_3 is having to compete with itself by giving electrons but is also pulling away due charge density due to the partial negative on the oxygen thus making the 2-phenoxypyridine a slightly weaker nucleophile compared to when it only has the CH_3. Overall it can be said that when electron withdrawing groups are present at the *meta* position on the 2-phenoxypyridine the reaction rate is hindered due to the resonance effect induced by these substituents.

Figure 11 σ⁻ Hammett Plot for *m*-substituted 2-phenoxypyridines
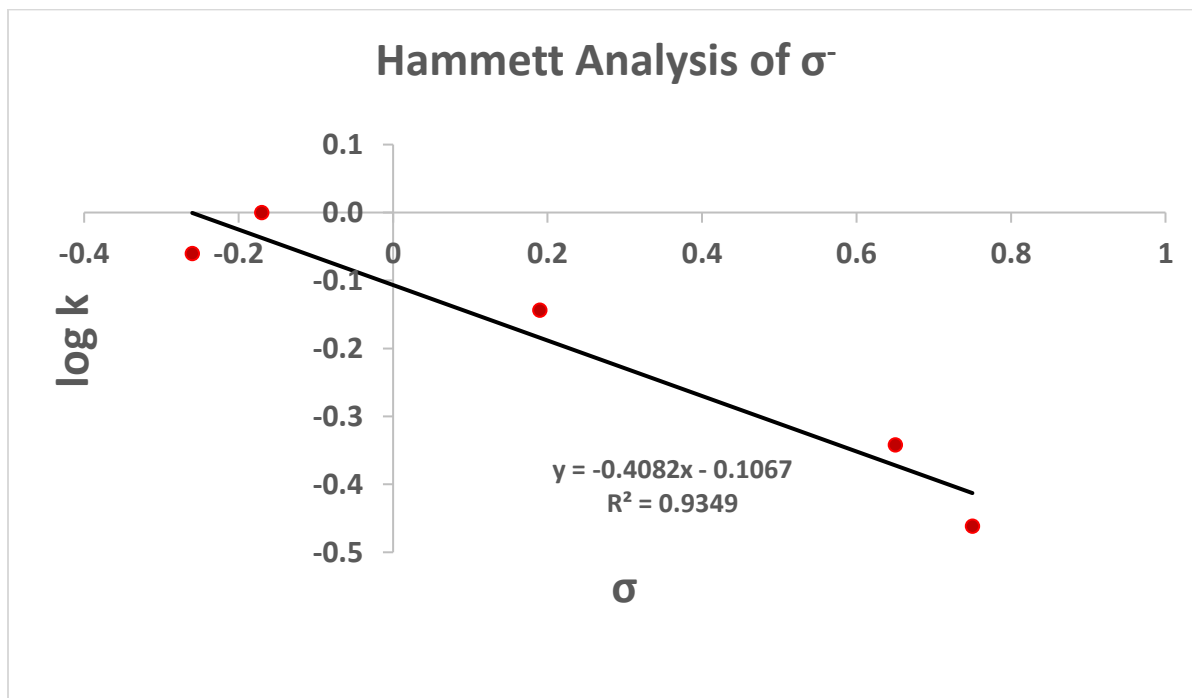
Para Substituents

Following the *meta* Hammett analysis the *para* substituents were then tested. A competing reaction was performed with various *para*-substituted 2-phenoxypyridines against an unsubstituted standard (**Scheme 18**). Diacylation occurs when the *para* position of the 2-phoxypyridine is substituted thus *p*-H was able to be used as the standard for the competing reaction.

Scheme 18 Competing reaction for *p*-Substituted 2-phenoxypyridines
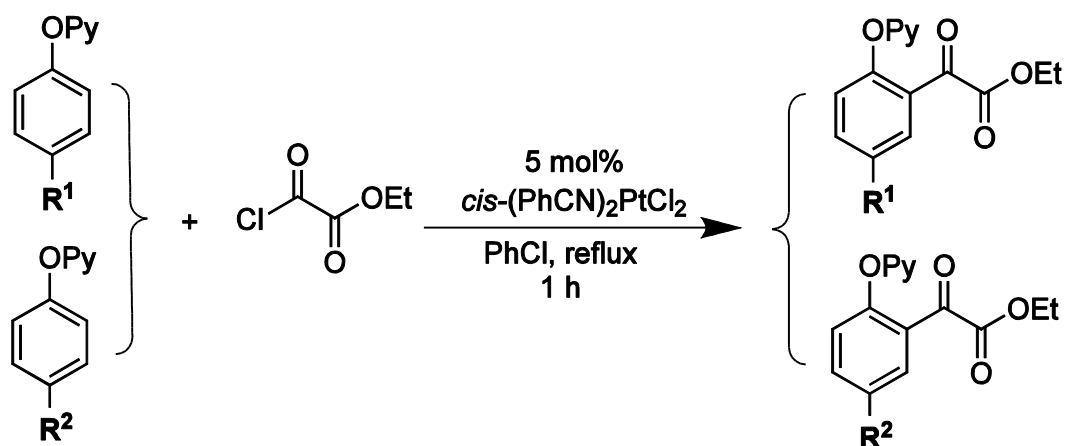
R¹=H
R²=OCH₃, CH₂CH₃, CO₂Et, Br

Following the completion of the competing reaction ^{1}H NMR was performed on each of the sample pulls. Unfortunately, with the use of the *p*-H standard 1H NMR elucidation became more difficult than when examining the *meta* substituents due to the similarity of various product's various aromatic regions. When it was not possible to identify unique peaks to each structure *p*-OMe was used as comparison with the values then being normalized to the *p*-H. This was done by taking the reaction ratio for the *p*-OMe and p-H multiplying it by the inverse of the reaction ratio for the *p*-OMe and the *p*-substrate of interest. For example, the relative rate for the

comparison of p-Br vs. p-H was determined as kBr/kH = kBr/kOme • kOMe/kH = 0.543• 0.862= 0.47. Standard deviations were calculated by performing the same analysis above on each of the reaction pulls (0, 5, 10 min…. etc.). **Figure 12** represents the full spectra for p-H vs. p-OMe and **Figure 13** is the expanded version to demonstrate compound identification of the sample withdrawn at 20 min of reaction. The resulting peaks were equalized to 0.5 mmol and the resulting ratios were plugged into the Ingold-Shaw expression with the resulting value found in **Table 6**. It is worth noting that the p- CO_2Et was tested as well but shared too many signals to both standards thus its data had to be omitted.

Figure 12 1H NMR of crude reaction mixture at 20 min from competing reaction of p-OCH_3 vs. p-H
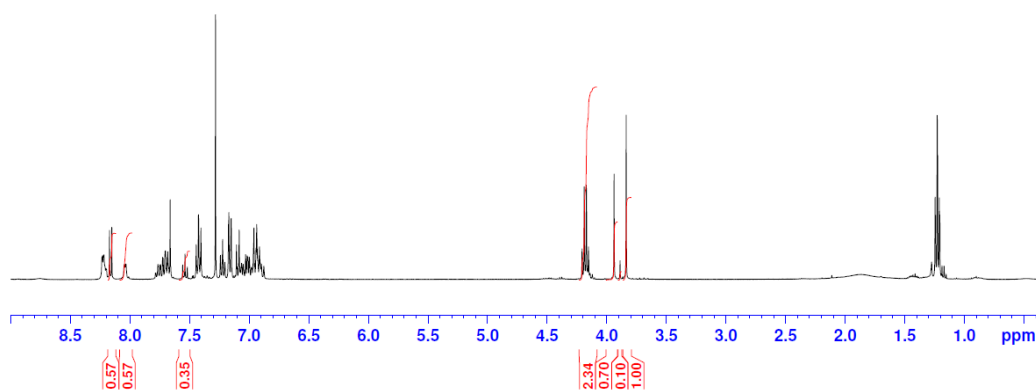
20 min

Figure 13 Expanded 1H NMR of crude reaction mixture at 20 min from competing reaction of *p*-OCH₃ vs. *p*-H

20 min
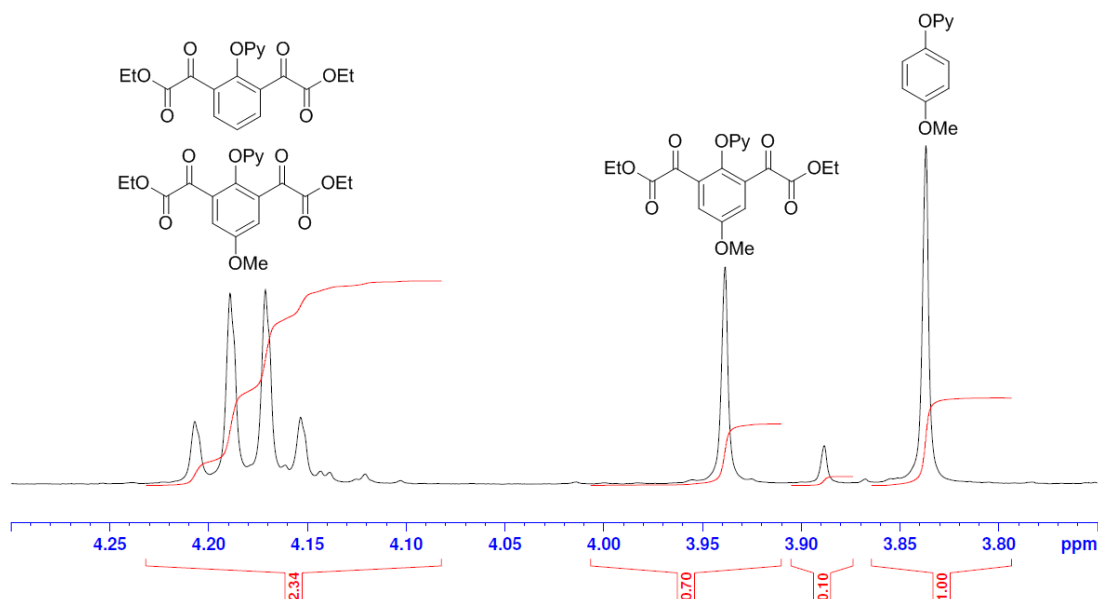
Much like in the *m*-Hammett 1H NMR mentioned prior, the only peak that was able to consistently be used for the *para* analysis was the keto ester shift (4.15 ppm). This was because for most of the products the shifts overlapped at different times and could not be used for consistent analysis. One unforeseen consequence for this is that the overall accuracy of the experiment is significantly lower than that of the *meta.* This loss of accuracy is due to the presence of mono-substituted product that is also formed during the reaction. This mono substituted product shares similar shifts to that of the product and provides a significant amount of interference when attempting this analysis. Due to the overall difficulty in isolating pure monosubstituted product no sample spectra were obtained as standards thus the significance of the interference is unknown. When looking at the *p*-OMe a small peak appears in-between the

49

starting material peak and the product peak. It is possible that this peak represents this substrate monosubstituted product, but it is not clear how much of the other substrate has monosubstituted.

Table 6 Ingold-Shaw rate constants for the competition of various *p*-substrates vs. a *p*-H standard OMe vs. CH_2CH_3/Br normalized to *p*-H standard

Substituent	OMe	H
OMe		0.86±0.004
Et	1.170±0.099	0.74±0.023
H		1.00±0.000
Br	1.84±0.169	0.47±0.015

[a] General conditions: Substituted 2-phenoxypyridine (0.5 mmol), Unsubstituted 2-phenoxypyridine (0.5 mmol), ethyl chlorooxoacetate (1.0 mmol), cis-Pt(PhCN)$_2$Cl$_2$ (0.05 mmol) chlorobenzene (6 mL), reflux, samples taken at 0, 5, 10, 15, 20, 40, and 60 min.

Just like the *m*-Hammett analysis the resulting rate constants were plugged into the Hammett equation producing the values found in **Table 7** (Log k/k_{CH3}). The Hammett values were then plotted against their standard sigma values[30]

Table 7 *p*-Hammett values for substituted 2-(aryloxy)pyridines

Substituent	Sigma m	Sigma p	Sigma +	Sigma -	Log(k/kH)
CH2CH3	-0.07	-0.15	-0.3	-0.19	-0.132
Br	0.39	0.23	0.15	0.19	-0.328
OCH3	0.1	-0.27	-0.78	-0.26	-0.064
H	0	0	0	0	0

When performing the various Hammett analyses, it was found that there was a severe lack of linearity among all the plots (**Figure 14 - 17**). When each point was examined further it was found that they were lower than the unsubstituted 2-phenoxypyridine. The reason for this

error can be attributed to the loss of accuracy when performing the 1H NMR analysis previously mentioned. By not being able to accurately assign monosubstituted products skews the resulting ratios thus adding error into the Hammett analysis. This error is further exacerbated when considering the need to standardize to the unsubstituted 2-phenoxypyridine. Error in the standard spectra would spread to each of the resulting points. However, the errors present are consistent across each of the various points since they are standardized to the *p*-H. Thus, the resulting Hammett plots can still be used to derive general trends (positive or negative slope) but not go into specific reaction sensitivities (ρ value).

When plotting σ_{para} (**Figure 14**) and σ_{meta} (**Figure 15**) the main goal was to see how resonance and inductive effects play a role in the reaction. It was found that the slope for the respective plots were both negative indicating a positive charge build up at the reaction center. This result matches that seen with the *meta* substituents. It is possible that they experience the same effect. Both plots fail to have an acceptable linearity due to the error mentioned earlier however, when the outlier point (*p*-H) is removed the correlation for the σ_{para} increases from 0.47 to 0.99 with the σ_{meta} remaining the same (0.66). Though this correlation cannot be used as concrete evidence, this preliminary result demonstrates that the σ_{para} substrates are ultimately correlating better than the σ_{meta}, demonstrating a favorability towards resonance effects playing a role in the reaction mechanism at the *para* position. However, the previously mentioned errors would need to be alleviated before any definitive statements can be made.

Figure 14 σ_{para} Hammett Plot for *p*-substituted 2-phenoxypyridines
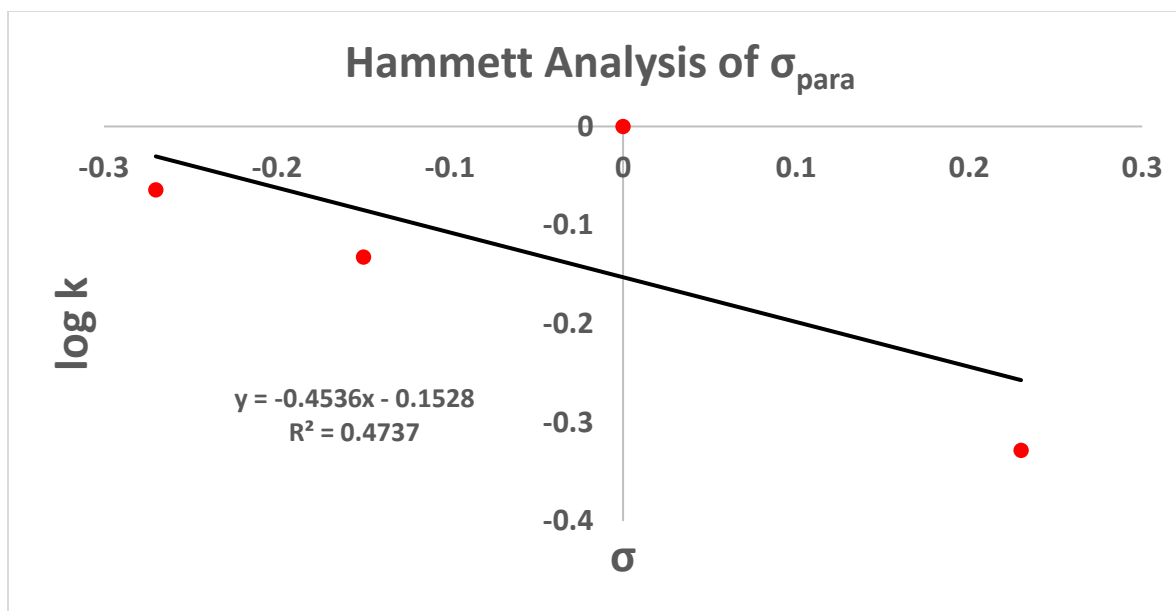
Figure 15 σ_{meta} Hammett Plot for *p*-substituted 2-phenoxypyridines
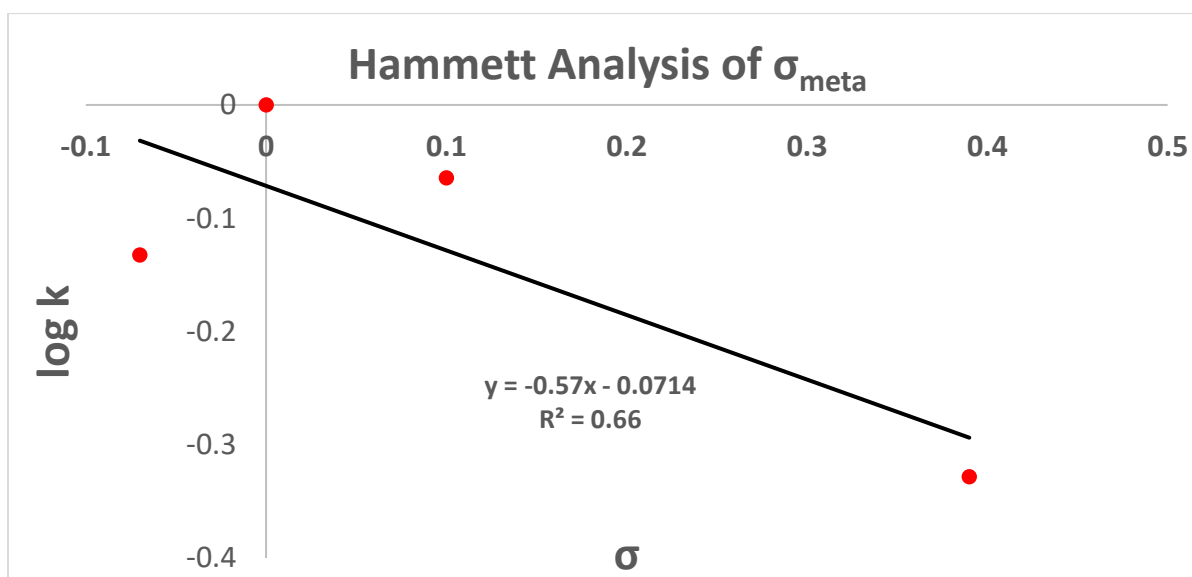
To probe further σ^+ and σ^- were both plotted to see how electron donating and electron withdrawing groups affect the reaction (**Figure 16 & 17**). Both plots failed to have acceptable linearity due for the same reasons previously mentioned. Both plots exhibited a negative slope keeping the trend that there is a positive charge build up at the reaction center. The same outlier point was eliminated for both plots. When this point was eliminated the correlation increased for

both Hammett plots (σ^+ 0.22-0.92 and σ^- 0.40- 0.99). These correlations point the possibility that

the electron withdrawing groups are playing a similar role to that of the *meta* substituents. It is

possible that the Br is pulling electron density away through inductive effect thus lowering the

rate of reaction due to the weakening of the nucleophile. It is also possible that the OMe is

performing a similar role through its slight inductive effect. It is interesting to note that the

electron donating groups are attributing more to the resonance effect at the *para* position then at

the *meta* position indicated by faster relative rates of the OMe compared to the Et. However,

more substrates would need to be tested to further probe these effects. These results help identify

the charge build up and demonstrate the same slowing seen in the *meta*-analysis. This indicates

that as electron density is removed, the nucleophile is still weakening slowing the reaction with

the inverse being said as electron density is pumped into the substrate. Once the issues

mentioned earlier are alleviated and more substrates are analyzed a better Hammett Plot can be

derived and more mechanistic insight can be obtained.

Figure 16 σ^+ Hammett Plot for *p*-substituted 2-phenoxypyridines
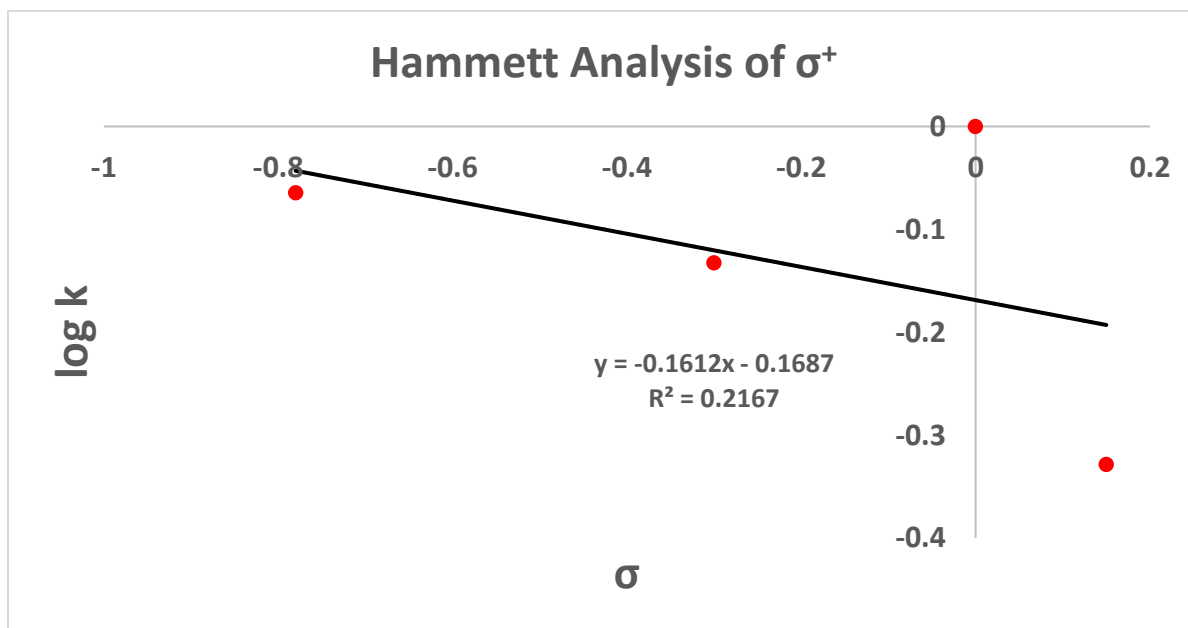
Figure 17 σ⁻ Hammett Plot for *p*-substituted 2-phenoxypyridines
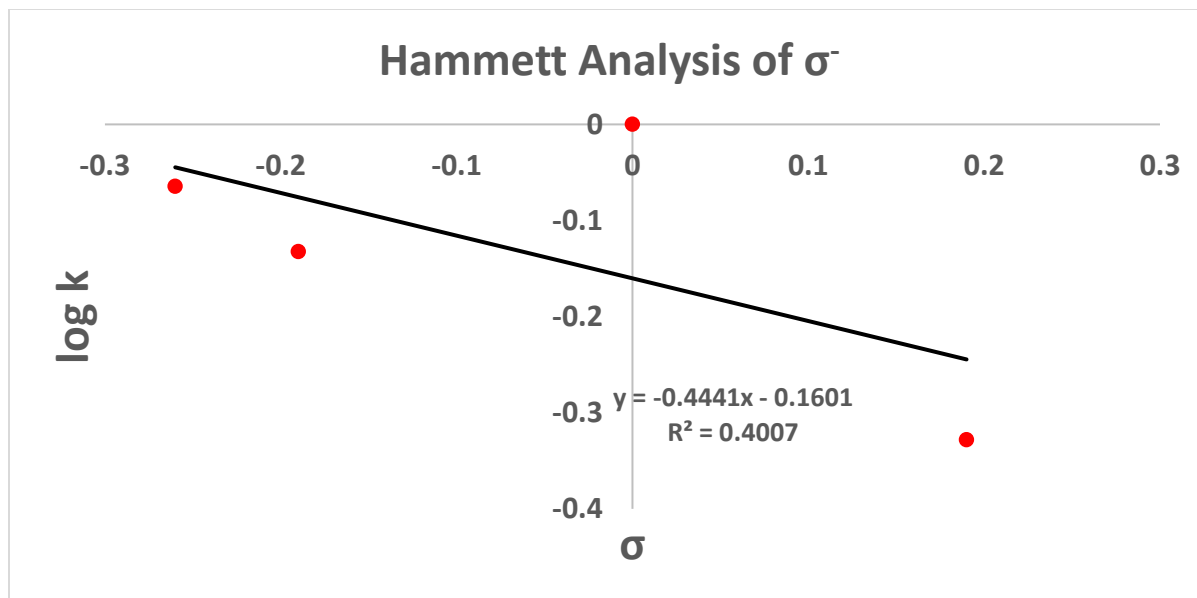
5.4 Experimental Section

All reactions were carried out under argon atmosphere and anhydrous conditions. All anhydrous solvents used were purchased from Aldrich Chemical Co. with Sure Seal and used as received. The *cis*-Pt(PhCN)$_2$Cl$_2$, was prepared according to literature procedures[4]. Ethyl chlorooxoacetate was purchased from Sigma Aldrich and was used as received. Thin layer chromatography was performed with silica gel 60 F254 plates, purchased from EMD chemicals. ^{1}H spectra were recorded on a Bruker 400 MHz spectrometer at 298K using CDCl$_3$.

General Procedure for Competing Pt-catalyzed Acylation Reaction

A 50 mL, three-necked round-bottom flask with a condenser was dried and charged with argon, and then charged with 2-(3-methylphenoxy)-pyridine (92.62 mg, 0.5 mmol), 2-(3-methoxyphenoxy)-pyridine (100.5 mg, 0.5 mmol), cis- (PhCN)$_2$PtCl$_2$ (23.9 mg, 0.05 mmol), ethyl chlorooxoacetate (0.11 ml, 1.0 mmol), and anhydrous chlorobenzene (6 mL). The mixture

was stirred and heated at reflux for 1 h. Aliquots were taken at varying time intervals (0.3 mL 0, 5, 10, 15, 20, 40, 60 min) and added to a 40 mL test tube under argon. Pyridine (0.1 mL) was added to the solution and heated (100 °C) for 10 min to free any products and unreacted starting materials that remained coordinated to the platinum. The mixture was transferred to a 30 ml separatory funnel, ethyl acetate (3 ml) was added, and the organic layer was washed with H_2O (3 x1 mL). The resulting organic layer was then concentrated via rotary evaporator followed by Oil Pump. The resulting mixtures were analyzed via ^{1}H NMR to identify both starting materials and their respective acylated products. Analysis was done using previously reported standards[34] for signal identification and quantification. Ingold-Shaw analysis was then applied to the resulting ^{1}H NMR data. Hammett values were then derived from this data.

5.5 Mechanistic Insight Obtained

It was found at the conclusion of this investigation that *meta* and *para* substituted 2-phenoxypyridines are highly affected by resonance effects exhibited by electron withdrawing substituents (σ^-). Insight gained from the Hammett analysis demonstrates a more complex mechanism than previously proposed. The slope of the graph demonstrates a positive charge build up however, the strong correlation to σ^- indicates direct resonance interaction with an anion reaction center. A possible explanation is the substituent effect may be more significant on the platinum than the 2-(aryloxy)pyridine. The Pt could serve as the nucleophile to attack the electrophiles (acyl chloride or acylium ion) instead of the electrophile attacking the ring. However, it is also possible that the positive charge present in the proposed mechanism does not exist for a significant amount of time in the reaction mechanism. This charge is potentially spread across the metalated carbon and the bridging carbon causing a partial positive build up at the reaction site, thus allowing for the introduction of the electrophile (**Scheme 8**). This sharing

of charge can also account for why the *meta* and *para* substituents yielded similar results. When electron withdrawing groups are present at the *meta* and *para* positions the resonance effects pull electron density away from the reaction center weakening the nucleophile thus causing a reduction in the rate of the reaction indicated by the σ^- Hammett plot. This interaction can also account for why very strong electron withdrawing groups such as NO_2 hinder the reaction all together. When the reaction site is too electron deficient the electrophile is unable to bind, thus sinking the reaction. Inversely, electron donating groups can speed up the reaction for a similar reason. However, it is important to note that at the *meta* position OMe is inductively electron withdrawing but gives electron density through its resonance effect. This explains why the CH_3 had a faster rate of reaction. When the OMe substituent is at the *para* position, the inductive effect is not as strong as demonstrated by a faster rate than the CH_2CH_3 substituent. This could demonstrate an uneven charge distribution among the two partial positives favoring *para* substituents. However, conclusive explanation may not be practical due to the complexity of the Pt-catalyzed C-H acylation. It is very possible the reaction involves a number of steps/reactions, coordination/ligand exchange, complex C-H activation or different acylation processes that are not present in the current proposed reaction mechanism. Computational studies paired with more substrate tests are needed to fully elucidate the substituent effects on the reaction.

CHAPTER 6: CONCLUSIONS

This research has further expanded the scope of the Pt-catalyzed acylation of 2-(aryloxy)pyridines and explored into the reaction mechanism. Through the use of K_2CO_3 the overall catalytic load has been cut in half (10 mol% -5 mol%) effectively reducing the overall cost by 50% with comparable yields. By neutralizing strong acid build up during the reaction the $(PhCN)_2PtCl_2$ catalyst is able to undergo a more effective catalytic cycle due to lack of competition for substrate binding otherwise experienced without a base. The reaction scope has been further expanded through the successful synthesis of the γ-keto ester. It was found that despite the addition of the two carbon spacer between the keto and ester functional groups the reagent was still able to acylate despite it being a weaker electrophile compared to the α-keto esters. The γ-keto esters were highly sensitive to electronic effects at the *meta* and *para* positions with strong electron withdrawing groups preventing acylation from occurring. The Pt-catalytic protocol did not work for the synthesis of a β-keto ester with ethyl malonyl chloride as the acylating reagent under the same conditions.

Substitution effects were explored through the use of Hammett analysis. It was found that *meta* and *para* substituted 2-(aryloxy)pyridines had the strongest correlation with σ^-, resulting in a negative slope. This result demonstrates that a positive charge is built up in the reaction, however, there is also an interaction with an anion reaction center. It is proposed that the Pt is acting as the nucleophile in the reaction due to the available d electrons present on the metal. From this finding it can be hypothesized that as the electron withdrawing groups pull more electron density away, the substrate becomes a poorer nucleophile due to the increase in positive charge build up (or loss of negative charge) at the acylation site. Thus explaining why strong electron withdrawing groups like NO_2 prevent acylation.

Future work for this project includes further reduction of catalytic loading through the synthesis of a more effective Pt(II) catalyst and further exploration into the role bases play in the acid neutralization. The reaction scope of γ-keto esters needs to be further explored through more substrates. Computational studies paired with further substrate testing are needed to further elucidate the role substituents play in the reaction and how varying substituents affect overall charge distribution.

REFERENCES

1. Labinger, J; Platinum-Catalyzed C-H Functionalization. *Chem. Rev.* **2017**, *117*, 8483-8496.

2. Ali, I; Waseem A.;Saleem, K.; Haque A. Platinum Compounds: A Hope for Future Cancer Chemotherapy. *Anti-Cancer Agents in Med. Chem.* **2013**, *13*, 296-306.

3. Zhu, H.; Ziegler, T. Influence of Cis and Trans Ligands in Platinum(II) Complexes on the Ability of the Platinum Center to Activate C−H Bonds. A Density Functional Theory Study. *Organometallics* **2008**, *27*, 1743-1749.

4. McAteer, D. C.; Javed, E.; Huo, L.; Huo, S. Platinum-Catalyzed Double Acylation of 2-(Aryloxy)pyridines via Direct C-H Activation. *Org. Lett.* **2017**, *19*, 1606-1609.

5. Raj, J. G. J.; Pathak, D. D.; Kapoor, P. N. Multi-Nuclear NMR Investigation of Nickel(II), Palladium(II), Platinum(II) and Ruthenium(II) Complexes of an Asymmetrical Ditertiary Phosphine. *J. Korean Chem. Soc.* **2013**, *57*, 726-730.

6. Anderson, K. M.; Orpen, A. G. On the relative magnitudes of cis and trans influences in metal complexes. *Chem. Commun.* **2001**, 2682-2683.

7. Lewis, L. Alleyne Selective synthesis of cis- and trans-[(NHCMe)2- PtCl2] and [NHCMePt(cod)Cl][NHCMePtCl3] using NHCMeSiCl4†. *Dalton Trans*., **2014**, *43*, 15700-15702

8. Argyle, M.; Bartholomew, C. Heterogeneous Catalyst Deactivation and Regeneration: A Review. *Catalysts* **2015**, *5*, 145-269.

9. Crabtree, R. H.; Lei, A. Introduction: CH Activation. *Chem. Rev.* **2017**, *117*, 8481-8482.

10. Shilov, A. E.; Shul'pin, G. Activation of C-H bonds by metal complexes. *Chem. Rev.* **1997**, *97*, 2879-2932.

11. Xia, Z.; He, C.; Wang, X.; Duan, C. Modifying electron transfer between photoredox and organocatalytic units via framework interpenetration for β-carbonyl functionalization. *Nat. Commun.* **2017**, *8*, 361.

12. Wu, X. Acylation of (Hetero)Arenes through C-H Activation with Aroyl Surrogates. *Chem. Eur. J.* **2015**, *21*, 12252-12265.

13. Lersch, M.; Tilset, M. Mechanistic Aspects of C—H Activation by Pt Complexes. *ChemInform* **2005**, *36*.

14. Furukawa, T.; Tobisu, M.; Chatani, N. C-H functionalization at sterically congested positions by the platinum-catalyzed borylation of arenes. *J. Amer. Chem. Soc.* **2015**, *137*, 12211-12214.

15. H. Annita Zhong; Jay A. Labinger; John E. Bercaw.; C-H Bond Activation by Cationic Platinum(II) Complexes: Ligand Electronic and Steric Effects. *J. Amer. Chem. Soc*. **2002**, *124*.

16. Uchiyama, T.; Nakamura, Y.; Miwa, T.; Kawaguchi, S.; Okeya, S. cis- and trans-dichlorobis(benzonitrile)platinum(II): preparation and isomerization studies by ^{13}C NMR spectroscopy. *Chem. Lett.***1980**, *9*, 337-338.

17. Zhu, H.; Ziegler, T. Influence of Cis and Trans Ligands in Platinum(II) Complexes on the Ability of the Platinum Center to Activate C−H Bonds. A Density Functional Theory Study. *Organometallics* **2008**, *27*, 1743-1749.

18. Bensimon, C.; Thouin, E.; Rochon, F. D.; Melanson, R.; Beauchamp, A. L. Synthesis and study of Pt(II)-nitrile complexes. Multinuclear NMR spectra and crystal structures of compounds of the types [Pt(R-CN)Cl3]− and cis and trans-Pt(R-CN)2Cl2. *Can. J. Chem.* **1996**, *74*, 144-152.

19. Quintal, S. M. O.; Qu, Y.; Quiroga, A. G.; Moniodis, J.; Nogueira, H. I. S.; Farrell, N. Pyridine-carboxylate complexes of platinum. Effect of N,O-chelate formation on model bifunctional DNA-DNA and DNA-protein interactions. *Inorg. Chem.***2005**, *44*, 5247

20. Konnick, M. M.; Bischof, S. M.; Yousufuddin, M.; Hashiguchi, B. G.; Ess, D. H.; Periana, R. A. A mechanistic change results in 100 times faster CH functionalization for ethane versus methane by a homogeneous Pt catalyst. *J. Amer. Chem. Soc.***2014**, *136*, 10085-10094.

21. Yi, C. S.; Yun, S. Y. Scope and mechanistic study of the ruthenium-catalyzed ortho-C-H bond activation and cyclization reactions of arylamines with terminal alkynes. *J. Am. Chem. Soc.* **2005**, *127*, 17000.

22. Lehnherr, D.; Wang, X.; Peng, F.; Reibarkh, M.; Weisel, M.; Maloney, K. M. Mechanistic Study of a Re-Catalyzed Monoalkylation of Phenols. *Organometallics* **2019**, *38*, 103-118.

23. Boess, E.; Wolf, L. M.; Malakar, S.; Salamone, M.; Bietti, M.; Thiel, W.; Klussmann, M. Competitive Hydrogen Atom Transfer to Oxyl- and Peroxyl Radicals in the Cu-Catalyzed Oxidative Coupling of N-Aryl Tetrahydroisoquinolines Using tert-Butyl Hydroperoxide. *ACS Catal.* **2016**, *6*, 3253-3261.

24. Schimler, S. D.; Froese, R. D. J.; Bland, D. C.; Sanford, M. S. Reactions of Arylsulfonate Electrophiles with NMe4F: Mechanistic Insight, Reactivity, and Scope. *J. Org. Chem.* **2018**, *83*, 11178-11190.

25. Štefane, B.; Grošelj, U.; Svete, J.; Požgan, F.; Kočar, D.; Brodnik Žugelj, H. The Influence of the Quinoline Moiety on Direct Pd-Catalyzed Arylation of Five-Membered Heterocycles. *Eur. J. Org. Chem.* **2019**, *2019*, 432-441.

26. Hammett, L;The Effect of Structure upon the Reactions of Organic Compounds. Benzene Derivatives. *J. Am. Chem. Soc.* **1937**, *59*, 96-103.

27. Mondal, P.; Pirovano, P.; Das, A.; Farquhar, E. R.; McDonald, A. R. Hydrogen Atom Transfer by a High-Valent Nickel-Chloride Complex. *J. Am. Chem. Soc.* **2018**, *140*, 1834-1841.

28. Masumoto, Y.; Miyamoto, K.; Iuchi, T.; Ochiai, M.; Hirano, K.; Saito, T.; Wang, C.; Uchiyama, M. Mechanistic Study on Aryl-Exchange Reaction of Diaryl-λ3-iodane with Aryl Iodide. *J. Org. Chem.* **2018**, *83*, 289-295.

29.Figg, T; Cundari, T. Computational Hammett analysis of redox based oxy-insertion by Pt(II) complexes. *Dalton Trans.***2013**, *42*, 4114–4121

30. Hansch, C; A. Leo; R. W. Taft. A Survey of Hammett Substituent Constants and Resonance and Field Parameters. Chem. Rev. **1991**, *91,* 165-195

31. Nakanowatari S; Mei R; Feldt M; Ackermann L. Cobalt(III)-Catalyzed Hydroarylation of Allenes via C-H Activation. *ACS Catal.* **2017** *7 (4),* 2511-2515

32. Kerber, W. D.; Nelsen, D. L.; White, P. S.; Gagné, M. R. Synthesis and ligand exchange reactions of P2Pd(II) and P2Pt(II) salicylaldimates. *Dalton Trans.* **2005**, 1948-1951.

33. Ayyangar, N. R.; Srinivasan, K. V. Effect of substituents in the formation of diacetanilides. *Can. J. Chem.* **1984***, 62*, 1292-1296.

 34. Javed, E.; Guthrie, J; Chirayath, G. and Huo, S. Introducing an α-keto ester functional group through Pt-catalyzed direct C−H acylation with ethyl chlorooxoacetate **(2019)** *Unpublished Manuscript,* Department of Chemistry, East Carolina University, Greenville, North Carolina

35. Wang, S.; Yang, Z.; Liu, J.; Xie, K.; Wang, A.; Chen, X.; Tan, Z. *Chem. Commun*. **2012**, *48*, 9924-9926.

36. Brown H.;Wang K.;Scouten C. Hydroboration Kinetics: Unusual Kinetics for the Reaction of 9-Borabicyclo[3.3.1]nonane with Representative Alkenes. *Proc. Natl. Acad. Sci. U. S. A.* **1980***, 77*, 698-702.